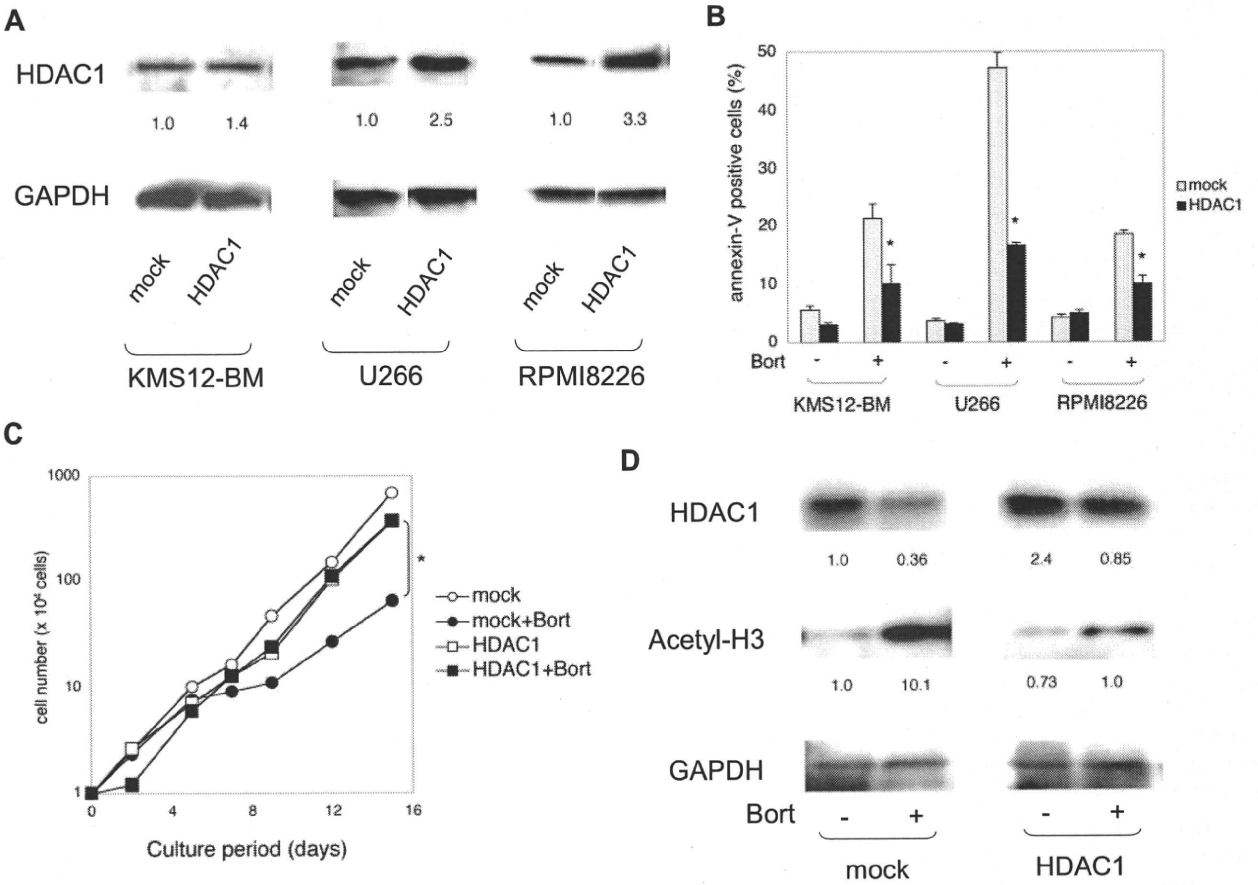

Figure 5. Effects of HDAC1 overexpression on bortezomib-induced apoptosis in MM cells in vitro. (A) MM cell lines were lentivirally transfected with CSII-DsRed (mock) or CSII-DsRed-HDAC1 (HDAC1) vector. Whole-cell lysates were prepared from DsRed$^+$ cells collected using a FACSAria flow cytometer and subjected to immunoblotting. The signal intensities of each band were quantified, normalized to those of the corresponding GAPDH, and shown as relative values with mock-transfected controls setting to 1.0. (B) MM cell lines transfected with mock or HDAC1 vector were cultured in the absence or presence of 2nM bortezomib. After 48 hours, MM cells were harvested, stained with annexin-V/APC, and subjected to flow cytometric analysis. The y-axis shows the proportion of annexin-V positivity in the DsRed$^+$ fraction. The means ± SD (bars) of 3 independent experiments are shown. *P* values were calculated by 1-way ANOVA with the Student-Newman-Keuls multiple comparisons test. *$P < .05$ against the mock. (C) RPMI 8226 cells transfected with mock or HDAC1 vector were cultured in the absence or presence of 2nM bortezomib. Total numbers of DsRed$^+$ cells were calculated by flow cytometer at the indicated time points. *P* values were calculated by 1-way ANOVA with the Student-Newman-Keuls multiple comparisons test. *$P < .05$ against the mock + Bort. (D) After 48 hours, whole-cell lysates were prepared from DsRed$^+$ cells collected using a FACSAria flow cytometer and subjected to immunoblotting. The signal intensities of each band were quantified, normalized to those of the corresponding GAPDH, and shown as relative values with untreated mock-transfected controls setting to 1.0.

indicate that the consequence of HDAC down-regulation is mainly apoptosis induction rather than growth inhibition. Histone hyperacetylation was enhanced by HDAC1 knockdown in bortezomib-treated RPMI8226 cells (Figure 4C). Therefore, it appears that shRNA-mediated knockdown of HDAC1 increases sensitivity to bortezomib via synergistic inhibition of HDAC activity in MM cells. These results suggest that bortezomib-induced cytotoxicity depends on cellular HDAC activities in MM cells.

HDAC1 overexpression rescues MM cells from bortezomib-induced apoptosis

To confirm the dependency of bortezomib action on HDACs, we performed gain-of-function of HDAC1 in MM cells using the lentiviral transduction system (supplemental Figure 6B).[27] CSII-DsRed (mock) and CSII-HDAC1-DsRed (HDAC1) vectors were lentivirally transduced into 3 MM cell lines. HDAC1 overexpression was confirmed by Western blotting in DsRed$^+$ cells collected by a cell sorter (Figure 5A). Using this system, we examined the effects of HDAC1 overexpression on bortezomib-induced apoptosis. As shown in Figure 5B, there was no significant difference in the proportion of apoptosis between mock- and HDAC1-transduced cells in the absence of bortezomib. In contrast, bortezomib-induced apoptosis was significantly inhibited by HDAC1 overexpression. The inhibition of apoptosis was observed in increased doses of bortezomib (supplemental Figure 8). However, overexpression of HDAC2 and HDAC3 did not ameliorate the effect of the drug (supplemental Figure 9), suggesting that the HDAC1 levels determine the sensitivity to bortezomib. Next, we investigated the effect of HDAC1 overexpression on the growth of bortezomib-treated cells. As shown in Figure 5C, there was no significant difference in the growth rate between mock- and HDAC1-transduced RPMI8226 cells in the absence of bortezomib. In the presence of bortezomib, the growth of mock-transduced cells was significantly delayed due to the induction of apoptosis. In contrast, HDAC1-transduced cells grew as fast as untreated cells, suggesting that HDAC1 overexpression ameliorates the cytotoxic effects of bortezomib. In addition, we examined the status of histone acetylation in these cells. As anticipated, HDAC1 overexpression markedly diminished bortezomib-induced hyperacetylation of histones (Figure 5D) but not tubulin (supplemental Figure 11). Taken together, HDAC1 overexpression rescued MM cells from bortezomib-induced apoptosis by sustaining HDAC activity in MM cells.

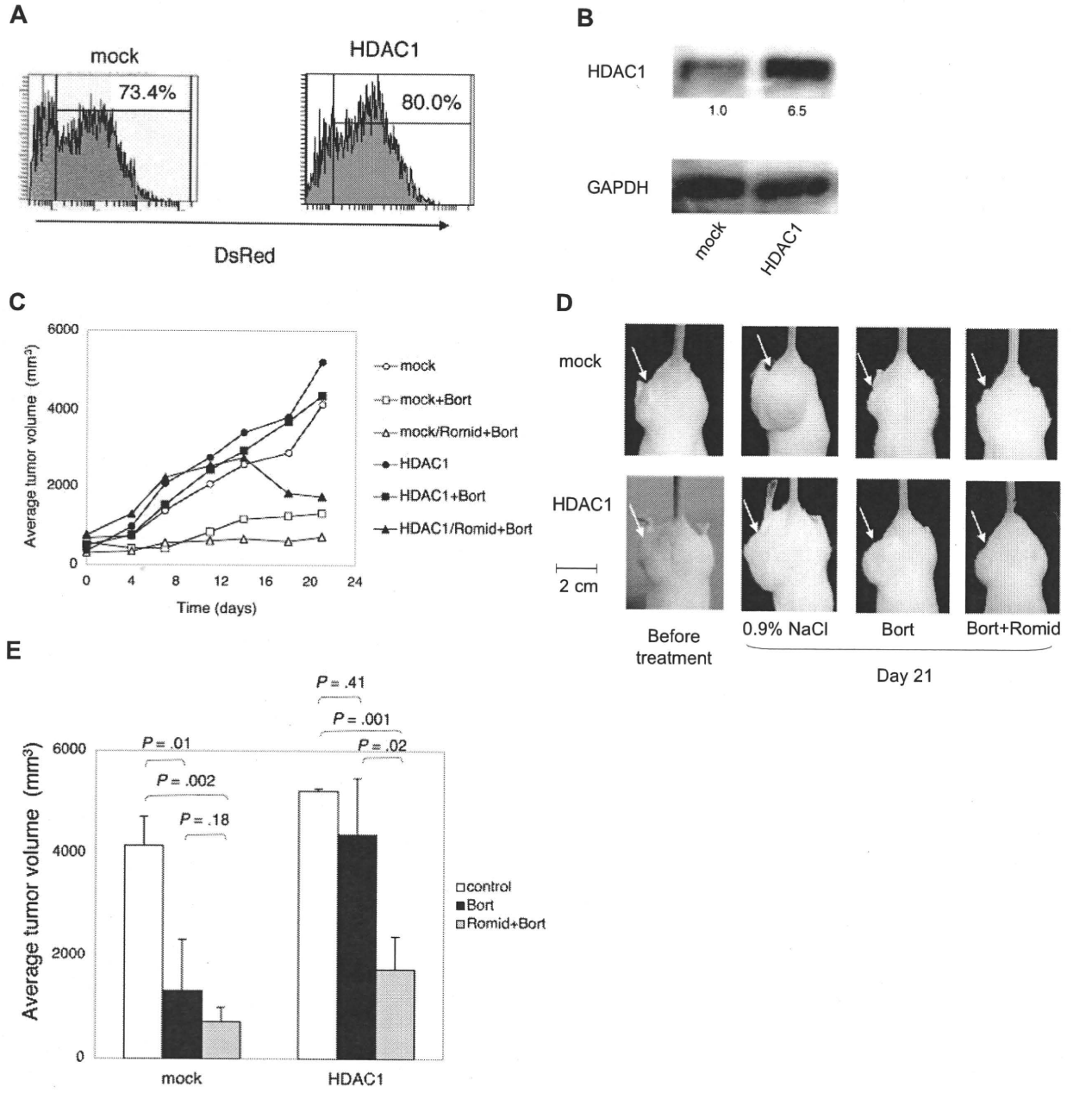

Figure 6. Effects of HDAC1 overexpression on bortezomib-induced apoptosis in RPMI 8226 cells in vivo. (A) RPMI 8226 cells were transfected with CSII-DsRed (mock) or CSII-DsRed-HDAC1 (HDAC1) vector. DsRed$^+$ cells were collected using a FACSAria flow cytometer and seeded 1 cell/well in a 96-well plate; single-cell clones were then obtained. Each subline was analyzed by a flow cytometer, and representative histogram plots of whole cells are shown. (B) Whole-cell lysates were subjected to immunoblotting. The signal intensities of HDAC1 were quantified, normalized to those of the corresponding GAPDH, and shown as relative values. (C) NOD/SCID mice were inoculated subcutaneously with 3×10^7 cells of RPMI 8226 sublines in the right thigh. The following treatments were started at day 0 when tumors were measurable: bortezomib intravenously twice a week, romidepsin intraperitoneally every other day, and vehicle (0.9% NaCl) alone at the same schedule. Caliper measurements of the longest perpendicular tumor diameters were performed on alternate days to estimate the tumor volume (mm^3) using the following formula: $4/3\pi \times (\text{width}/2)^2 \times (\text{length}/2)$. Mice inoculated with mock clones were treated with vehicle alone (mock; ○; n = 5), 0.5 mg/kg bortezomib (mock + Bort; □; n = 4), or 0.5 mg/kg bortezomib and 0.25 mg/kg romidepsin (HDAC1/Romid + Bort; △; n = 4). Mice inoculated with HDAC1 clones were treated with vehicle alone (HDAC1; ●; n = 4), 0.5 mg/kg bortezomib (HDAC1 + Bort; ■; n = 3), or 0.5 mg/kg bortezomib and 0.25 mg/kg romidepsin (HDAC1/Romid + Bort; ▲; n = 4). (D) Representative photographs of inoculated NOD/SCID mice at day 21 are shown (original magnification, ×2). Arrowheads indicate inoculated tumors. (E) The y-axis shows the tumor volume in inoculated mice at day 21. The means ± SD (bars) are shown. *P* values were calculated by 1-way ANOVA with the Student-Newman-Keuls multiple comparisons test.

Bortezomib resistance of HDAC1-transduced MM cells in NOD/SCID mice

Finally, we confirmed the role of HDACs as target molecules of bortezomib in vivo. To this end, we established RPMI 8226 sublines lentivirally transduced with CSII-DsRed (mock) or CSII-HDAC1-DsRed (HDAC1). Whereas each subline expressed DsRed at equal levels (Figure 6A), HDAC1 was overexpressed solely in the HDAC1-transduced subline (Figure 6B). We inoculated them subcutaneously into nonobese diabetic/severe combined immunodeficiency (NOD/SCID) mice in the right thigh at 3×10^7 cells.[31] When measurable tumors developed after 10 to 14 days, mice were assigned to 3 groups: vehicle (0.9% NaCl) control, 0.5 mg/kg bortezomib–treated, and 0.25 mg/kg romidepsin and 0.5 mg/kg bortezomib–treated (n = 3-5 in each group). As shown in Figure 6C, tumor volume constantly increased in vehicle control mice given transplants of both mock and HDAC1 until 21 days. Bortezomib strikingly inhibited tumor growth in mice

inoculated with mock-transduced cells, but failed to do so when HDAC1-transduced cells were inoculated. We compared the tumor volume between vehicle-control and bortezomib-treated groups on day 21. As shown in Figure 6D and E, the tumor volume of mock-transduced cells was significantly lower in the bortezomib-treated group than in the vehicle-control group. In contrast, there was no difference in the tumor volume of HDAC1-transduced cells between groups. These results suggest that HDAC1 overexpression confers bortezomib resistance to MM cells in vivo. To confirm the role of HDAC1 in bortezomib resistance, we examined the effects of an HDAC inhibitor on the sensitivity of HDAC1-transduced cells to bortezomib. The addition of romidepsin successfully regressed bortezomib-resistant tumor after 12 days (Figure 6C), and the tumor size was significantly smaller than that of the bortezomib-treated group at 21 days (Figure 6D-E). These results strongly suggest that HDACs are critical targets of bortezomib in vivo.

Discussion

In this study, we have clearly demonstrated that HDACs play a critical role in bortezomib-induced cytotoxicity against MM. The expression of class I HDACs was down-regulated by bortezomib at a transcriptional level via caspase-8–dependent degradation of Sp1 protein, the most potent transactivator of HDACs. As a result, HDAC activities were reduced in MM cells, leading to apoptotic cell death. Because Sp1 is a broadly acting transcription factor, many other target genes should be repressed by Sp1 down-regulation in bortezomib-treated MM cells. Using loss-of-function and gain-of-function analyses, however, we confirmed that sensitivity to bortezomib depends on the levels of HDAC1 expression in MM cells both in vitro and in vivo. This implies that HDACs are critical targets of Sp1 for bortezomib-induced cytotoxicity, although the involvement of other molecules cannot be ruled out. Taken together, our present findings may address the emerging question about the targets of bortezomib,[24] add a novel and critical determinant in a list of effector molecules of bortezomib,[42] and thus provide a novel rationale for the use of proteasome inhibitors in the treatment of patients with MM.

In support of our findings, recent evidence has suggested a close link between proteasome inhibitors and HDACs. Catley et al[43] reported that a hydroxamic acid–derivative NVP-LAQ824, referred to an HDAC inhibitor, affects proteasome activities in MM cells. This compound has a unique ability in overcoming cell adhesion–mediated drug resistance (CAM-DR) of MM cells. Recently, we have shown that VLA-4 is a key molecule of CAM-DR in MM cells, and bortezomib can overcome CAM-DR via the down-regulation of VLA-4 expression.[30] However, our preliminary experiments suggested that HDAC inhibitors, such as romidepsin and valproic acid, did not down-regulate VLA-4 expression but reversed CAM-DR in MM cells (data not shown). The characteristics of NVP-LAQ824 may not be like other HDAC inhibitors but rather resemble bortezomib; therefore, it is possible that NVP-LAQ824 inhibits HDAC activity via the down-regulation of HDAC expression. In addition, Miller et al[44] reported that a novel proteasome inhibitor NPI-0052 induced caspase-8–dependent histone acetylation in leukemia cells. They demonstrated that ubiquitinated histones did not accumulate in response to NPI-0052, indicating that histone hyperacetylation is not solely due to the accumulation of acetylated histones. It is likely that NPI-0052 induces HDAC down-regulation and histone hyperacetylation via the same mechanism as bortezomib, because we have found that bortezomib down-regulated HDAC expression not only in MM cells but also in other hematologic malignant cell lines, such as HL-60 (acute myeloid leukemia), BJA-B (Burkitt lymphoma) and K562 (chronic myelogenous leukemia; data not shown). Therefore, proteasome inhibitors may generally reduce HDAC activity via the down-regulation of HDAC expression in hematologic malignancies. On the other hand, Fotheringham et al[45] reported that HR23b, which shuttles ubiquitinated cargo proteins to the proteasome, is a mediator of HDAC inhibitor–induced cytotoxicity. HDAC inhibitors increased the activity of HR23b and provoked abnormal protein turnover, which resulted in the inhibition of proteasome activities by saturating the proteasome. Furthermore, Mitsiades et al[5,46] screened for target molecules of the HDAC inhibitor SAHA and bortezomib using DNA microarrays. Several molecules (p21, CXCR4, syndecan-1, IGF-1, cyclin B2, cyclin F, and bcl-2) are commonly influenced by SAHA and bortezomib in MM cells. Therefore, HDAC inhibitors and proteasome inhibitors may exert cytotoxicity through overlapping or redundant pathways.

Previous studies showed that the unfolded protein response is a dominant mechanism of bortezomib-induced cytotoxicity.[47] In this study, we have demonstrated that caspase-12 inhibitor, which could inhibit endoplasmic reticulum (ER) stress-induced apoptosis, did not affect bortezomib-induced apoptosis, but caspase-8 inhibitor did (Figure 3G). The caspase-8–mediated pathway is dominant more than the ER stress-mediated pathway in our system. This discrepancy may be attributable to the difference in doses of bortezomib; less than 8nM in our experiments versus more than 10nM in previous studies. Pharmacodynamic studies revealed that serum concentrations of bortezomib decrease to 2 ng/mL (approximately 5nM) or less 4 hours after administration of 1.3 mg/m^2 bortezomib.[48] Therefore, our data may reflect the cellular events in vivo more accurately, and support the notion that the caspase-8/Sp1/HDAC axis is more important than other pathways.

In recent clinical studies, bortezomib proved effective even in the context of heavily pretreated, relapsed and refractory MM; however, primary and secondary bortezomib resistance occurred in more than 50% of patients.[4] The molecular bases of different individual responsiveness to bortezomib remain unclear. Several previous studies have suggested that adaptation or sensitivity to bortezomib depends on the activity of the ubiquitin-proteosome system in MM cells.[49,50] We have demonstrated here that the overexpression of HDAC1 induced bortezomib resistance in vitro and in vivo. The current study is the second to demonstrate that adaptation to bortezomib can indeed be achieved in an MM cell line. Because of the variation of HDAC expression levels, the treatment outcome of bortezomib-treated patients may depend on HDAC activities of MM cells. Importantly, we could overcome the resistance to bortezomib by the combination of the HDAC inhibitor romidepsin in murine xenograft models. HDAC inhibitors, such as romidepsin, SAHA, and tubacin, are promising agents for patients with bortezomib-resistant MM for the following reasons: (1) bortezomib specifically down-regulated the expression of class I HDACs; (2) romidepsin inhibited both class I and II HDAC activities; and (3) HDAC6 knockdown enhanced bortezomib-induced apoptosis (supplemental Figure 10). Therefore, bortezomib is an indispensable agent for MM treatment and combination with other drugs, especially HDAC inhibitors, may be the best treatment strategy for MM treatment. Our findings reinforce the potential clinical utility of combining these 2 agents.

Acknowledgments

We are grateful to Drs Ralph Mazitschek and Stuart L. Schreiber (Broad Institute of Harvard University and Massachusetts Institute of Technology) for providing tubacin and niltubacin. We thank Ms Akiko Yonekura for excellent technical assistance.

This work was supported in part by the High-Tech Research Center Project for Private Universities: Matching Fund Subsidy from MEXT 2002-2006. J.K., T.W., K.N.-H., and K.M. are winners of the Jichi Medical School Young Investigator Award.

Authorship

Contribution: J.K. designed and performed experiments, analyzed data, and drafted the manuscript; T.W., R.S., M.A., K.M., and M.N. performed experiments; T.I. and Y.K. provided clinical samples; K.N.-H. and K.O. provided materials and critically reviewed the manuscript; and Y.F. designed and supervised research and wrote the manuscript.

Conflict-of-interest disclosure: The authors declare no competing financial interests.

Correspondence: Yusuke Furukawa, Division of Stem Cell Regulation, Center for Molecular Medicine, Jichi Medical University, 3311-1 Yakushiji, Shimotsuke, Tochigi 329-0498, Japan; e-mail: furuyu@jichi.ac.jp.

References

1. Kyle RA, Gertz MA, Witzig TE, et al. Review of 1027 patients with newly diagnosed multiple myeloma. *Mayo Clin Proc.* 2003;78(1):21-33.
2. Minucci S, Pelicci PG. Histone deacetylase inhibitors and the promise of epigenetic (and more) treatments for cancer. *Nat Rev Cancer.* 2006; 6(1):38-51.
3. Richardson PG, Mitsiades C, Schlossman R, et al. Bortezomib in the front-line treatment of multiple myeloma. *Expert Rev Anticancer Ther.* 2008; 8(7):1053-1072.
4. Richardson PG, Sonneveld P, Schuster M, et al. Extended follow-up of a phase 3 trial in relapsed multiple myeloma: final time-to-event results of the APEX trial. *Blood.* 2007;110(10): 3557-3560.
5. Mitsiades CS, Mitsiades NS, McMullan CJ, et al. Transcriptional signature of histone deacetylase inhibition in multiple myeloma: biological and clinical implications. *Proc Natl Acad Sci U S A.* 2004;101(2):540-545.
6. Sutheesophon K, Kobayashi Y, Takatoku MA, Ozawa K, Kano Y, Furukawa Y. Histone deacetylase inhibitor depsipeptide (FK228) induces apoptosis in leukemic cells by facilitating mitochondrial translocation of Bax, which is enhanced by the proteasome inhibitor bortezomib. *Acta Haematol.* 2006;115(1-2):78-90.
7. Badros A, Burger AM, Philip S, et al. Phase I study of vorinostat in combination with bortezomib for relapsed and refractory multiple myeloma. *Clin Cancer Res.* 2009;15(16):5250-5257.
8. Herman JG, Baylin SB. Gene silencing in cancer in association with promoter hypermethylation. *N Engl J Med.* 2003;349(21):2042-2054.
9. Marks P, Rifkind RA, Richon VM, Breslow R, Miller T, Kelly WK. Histone deacetylases and cancer: causes and therapies. *Nat Rev Cancer.* 2001;1(3):194-202.
10. Yang X-J, Seto E. The Rpd3/Hda1 family of lysine deacetylases: from bacteria and yeast to mice and men. *Nat Rev Mol Cell Biol.* 2008;9(3):206-218.
11. Lagger G, O'Carroll D, Rembold M, et al. Essential function of histone deacetylase 1 in proliferation control and CDK inhibitor repression. *EMBO J.* 2002;21(11):2672-2681.
12. Lin RJ, Nagy L, Inoue S, et al. Role of the histone deacetylase complex in acute promyelocytic leukemia. *Nature.* 1998;391(6669):811-814.
13. Wang J, Hoshino T, Redner RL, Kajigaya S, Liu JM. ETO, fusion partner in t(8;21) acute myeloid leukemia, represses transcription by interaction with the human N-CoR/mSin3/HDAC1 complex. *Proc Natl Acad Sci U S A.* 1998;95(18):10860-10865.
14. Kobayashi Y, Ohtsuki M, Murakami T, et al. Histone deacetylase inhibitor FK228 suppresses the Ras-MAP kinase signaling pathway by upregulating Rap1 and induces apoptosis in malignant melanoma. *Oncogene.* 2006;25(4):512-524.
15. Wada T, Kikuchi J, Nishimura N, Shimizu R, Kitamura T, Furukawa Y. Expression levels of histone deacetylases determine the cell fate of hematopoietic progenitors. *J Biol Chem.* 2009; 284(44):30673-30683.
16. Somech R, Izraeli S, J Simon A. Histone deacetylase inhibitors: a new tool to treat cancer. *Cancer Treat Rev.* 2004;30(5):461-472.
17. Kim DH, Kim M, Kwon HJ. Histone deacetylase in carcinogenesis and its inhibitors as anti-cancer agents. *J Biochem Mol Biol.* 2003;36(1):110-119.
18. Hideshima T, Richardson P, Chauhan D, et al. The proteasome inhibitor PS-341 inhibits growth, induces apoptosis, and overcomes drug resistance in human multiple myeloma cells. *Cancer Res.* 2001;61(7):3071-3076.
19. Soucy TA, Smith PG, Milhollen MA, et al. An inhibitor of NEDD8-activating enzyme as a new approach to treat cancer. *Nature.* 2009; 458(7239):732-736.
20. Chauhan D, Catley L, Li G, et al. A novel orally active proteasome inhibitor induces apoptosis in multiple myeloma cells with mechanisms distinct from Bortezomib. *Cancer Cell.* 2005;8(5):407-419.
21. Annunziata CM, Davis RE, Demchenko Y, et al. Frequent engagement of the classical and alternative NF-κB pathways by diverse genetic abnormalities in multiple myeloma. *Cancer Cell.* 2007; 12(2):115-130.
22. Keats JJ, Fonseca R, Chesi M, et al. Promiscuous mutations activate the noncanonical NF-κB pathway in multiple myeloma. *Cancer Cell.* 2007; 12(2):131-144.
23. Hideshima T, Chauhan D, Richardson P, et al. NF-kappa B as a therapeutic target in multiple myeloma. *J Biol Chem.* 2002;277(19):16639-16647.
24. Hideshima T, Ikeda H, Chauhan D, et al. Bortezomib induces canonical NF-kappa B activation in multiple myeloma cells. *Blood.* 2009;114(5): 1046-1052.
25. Drexler HG, Matsuo Y, MacLeod RA. Persistent use of false myeloma cell lines. *Hum Cell.* 2003; 16(3):101-105.
26. Furukawa Y, Vu HA, Akutsu M, et al. Divergent cytotoxic effects of PKC412 in combination with conventional antileukemic agents in FLT3 mutation-positive versus -negative leukemia cell lines. *Leukemia.* 2007;21(5):1005-1014.
27. Kikuchi J, Shimizu R, Wada T, et al. E2F-6 suppresses growth-associated apoptosis of human hematopoietic progenitor cells by counteracting proapoptotic activity of E2F-1. *Stem Cells.* 2007; 25(10):2439-2447.
28. Sutheesophon K, Nishimura N, Kobayashi Y, et al. Involvement of the tumor necrosis factor (TNF)/TNF receptor system in leukemic cell apoptosis induced by histone deacetylase inhibitor depsipeptide (FK228). *J Cell Physiol.* 2005; 203(2):387-397.
29. Furukawa Y, Kikuchi J, Nakamura M, Iwase S, Yamada H, Matsuda M. Lineage-specific regulation of cell cycle control gene expression during haematopoietic cell differentiation. *Br J Haematol.* 2000;110(3):663-673.
30. Noborio-Hatano K, Kikuchi J, Takatoku M, et al. Bortezomib overcomes cell-adhesion-mediated drug resistance through downregulation of VLA-4 expression in multiple myeloma. *Oncogene.* 2009;28(2):231-242.
31. LeBlanc R, Catley LP, Hideshima T, et al. Proteasome inhibitor PS-341 inhibits human myeloma cell growth in vivo and prolongs survival in a murine model. *Cancer Res.* 2002;62(17): 4996-5000.
32. Chen J, Zhang M, Ju W, Waldmann TA. Effective treatment of a murine model of adult T-cell leukemia using depsipeptide and its combination with unmodified daclizumab directed toward CD25. *Blood.* 2009;113(6):1287-1293.
33. Piekarz RL, Robey R, Sandor V, et al. Inhibitor of histone deacetylation, depsipeptide (FR901228), in the treatment of peripheral and cutaneous T-cell lymphoma: a case report. *Blood.* 2001;98(9): 2865-2868.
34. Byrd JC, Marcucci G, Parthun M, et al. A phase I and pharmacodynamic study of depsipeptide (FK228) in chronic lymphocytic leukemia and acute myeloid leukemia. *Blood.* 2005;105(3):959-967.
35. Hideshima T, Bradner JE, Wong J, et al. Small-molecule inhibition of proteasome and aggresome function induces synergistic antitumor activity in multiple myeloma. *Proc Natl Acad Sci U S A.* 2005;102(24):8567-8572.
36. Shi J, Tricot GJ, Garg TK, et al. Bortezomib down-regulates the cell-surface expression of HLA class I and enhances natural killer cell-mediated lysis of myeloma. *Blood.* 2008;111(3):1309-1317.
37. Liu S, Liu Z, Xie Z, et al. Bortezomib induces DNA hypomethylation and silenced gene transcription by interfering with Sp1/NF-kappaB-dependent DNA methyltransferase activity in acute myeloid leukemia. *Blood.* 2008;111(4):2364-2373.
38. Chimienti F, Seve M, Richard S, Mathieu J, Favier A. Role of cellular zinc in programmed cell death: temporal relationship between zinc depletion, activation of caspases, and cleavage of Sp family transcription factors. *Biochem Pharmacol.* 2001; 62(1):51-62.
39. Hideshima T, Mitsiades C, Akiyama M, et al. Molecular mechanisms mediating antimyeloma activity of proteasome inhibitor PS-341. *Blood.* 2003;101(4):1530-1534.
40. Thorpe JA, Christian PA, Schwarze SR. Proteasome inhibition blocks caspase-8 degradation and sensitizes prostate cancer cells to death receptor-mediated apoptosis. *Prostate.* 2008;68(2): 200-209.
41. Landowski TH, Megli CJ, Nullmeyer KD, Lynch RM, Dorr RT. Mitochondrial-mediated disregulation of Ca^{2+} is a critical determinant of Velcade (PS-341/bortezomib) cytotoxicity in myeloma cell lines. *Cancer Res.* 2005;65(9):3828-3836.
42. Dolcet X, Llobet D, Pallares J. NF-κB in development and progression of human cancer. *Virchows Arch.* 2005;446(5):475-482.
43. Catley L, Weisberg E, Tai YT, et al. NVP-LAQ824 is a potent novel histone deacetylase inhibitor

with significant activity against multiple myeloma. *Blood.* 2003;102(7):2615-2622.

44. Miller CP, Rudra S, Keating MJ, Wierda WG, Palladino M, Chandra J. Caspase-8 dependent histone acetylation by a novel proteasome inhibitor, NPI-0052: a mechanism for synergy in leukemia cells. *Blood.* 2009;113(18):4289-4299.
45. Fotheringham S, Epping MT, Stimson L, et al. Genome-wide loss-of-function screen reveals an important role for the proteasome in HDAC inhibitor-induced apoptosis. *Cancer Cell.* 2009;15(1):57-66.
46. Mitsiades N, Mitsiades CS, Poulaki V, et al. Molecular sequelae of proteasome inhibition in human multiple myeloma cells. *Proc Natl Acad Sci U S A.* 2002;99(22):14374-14379.
47. Obeng EA, Carlson LM, Gutman DM, Harrington WJ, Lee KP, Boise LH. Proteasome inhibitors induce a terminal unfolded protein response in multiple myeloma cells. *Blood.* 2006;107(12):4907-4916.
48. Ogawa Y, Tobinai K, Ogura M, et al. Phase I and II pharmacokinetic and pharmacodynamic study of the proteasome inhibitor bortezomib in Japanese patients with relapsed or refractory multiple myeloma. *Cancer Sci.* 2008;99(1):140-144.
49. Rückrich T, Kraus M, Gogel J, et al. Characterization of the ubiquitin-proteasome system in bortezomib-adapted cells. *Leukemia.* 2009;23(6):1098-1105.
50. Bianchi G, Oliva L, Cascio P, et al. The proteasome load versus capacity balance determines apoptotic sensitivity of multiple myeloma cells to proteasome inhibition. *Blood.* 2009;113(13):3040-3049.

Leukemia Research 34 (2010) 1057–1063

Contents lists available at ScienceDirect

Leukemia Research

journal homepage: www.elsevier.com/locate/leukres

Combination of tipifarnib and rapamycin synergistically inhibits the growth of leukemia cells and overcomes resistance to tipifarnib via alteration of cellular signaling pathways

Tadashi Nagai*, Ken Ohmine, Shin-ichiro Fujiwara, Mitsuyo Uesawa, Chihiro Sakurai, Keiya Ozawa

Division of Hematology, Department of Medicine, Jichi Medical University, 3311-1 Yakushiji, Shimotsuke, Tochigi, Japan

ARTICLE INFO

Article history:
Received 14 August 2009
Received in revised form
27 November 2009
Accepted 18 December 2009
Available online 13 January 2010

Keywords:
Tipifarnib
Farnesyltransferase inhibitor
Rapamycin
K562
K562/RR
Leukemia

ABSTRACT

Small molecules are attractive agents for the treatment of leukemia. We found that a combination of a farnesyltransferase inhibitor, tipifarnib, and an mTOR inhibitor, rapamycin, synergistically inhibited the growth of myeloid leukemia cell lines and primary leukemia cells by inducing apoptosis and cell-cycle blockage. The combined agents reduced the level of phospho-ERK1/2, suggesting that they altered the network of signaling pathways. They also showed synergistic effects in tipifarnib-resistant K562/RR cells. The results support the utility of this combination as a potential therapy for leukemia. The combination might also be effective in overcoming resistance to tipifarnib.

1. Introduction

Recent studies have revealed that deregulation of a variety of cellular signaling pathways and of the expression of genes that control cell proliferation, survival, apoptosis, and differentiation is involved in the development of leukemia. Recently, many kinds of small molecules aimed at restoring the regulation of these pathways have been developed and studied at preclinical or clinical levels for use in the treatment of leukemia [1]. The most successful examples of this strategy are trans-retinoic acid and BCR/ABL kinase inhibitors, including imatinib, nilotinib, and dasatinib, which show substantial clinical effects against acute promyelocytic leukemia and BCR/ABL-positive leukemia, respectively [2]. Unfortunately, many other small molecules have shown only limited efficacy for the treatment of leukemia in clinical studies, possibly because the accumulation of a variety of cellular abnormalities is involved in the development and progression of leukemia [3]; thus, treatment of leukemia with a single agent of small molecule weight can hardly overcome all of these abnormalities. There is, therefore, a need to develop effective combination therapies for clinical application.

Tipifarnib (Zarnestra™, Johnson & Johnson Pharmaceutical Research & Development, Titusville, NJ), a farnesyltransferase inhibitor, has been shown to inhibit the growth of tumor cells including leukemia cells *in vitro* [4]. Some cellular proteins require farnesylation to become active, and it is thought that tipifarnib suppresses the function of some oncogenic proteins by inhibiting farnesylation and thus, inhibiting abnormally activated signaling pathways. However, the results of clinical studies have shown that tipifarnib alone had only a moderate effect against various hematologic disorders [4–11]. In addition, acquisition of drug resistance is an important consideration in patients being treated with tipifarnib. In light of this, the development of efficacious combination therapies involving tipifarnib and other agents appears to be an attractive approach for making good use of tipifarnib in the treatment of leukemia. Indeed, previous studies have shown that combination therapy with tipifarnib and certain other drugs had synergistic or additive inhibitory effects on the growth of leukemia cells [12,13].

In this study, we examined *in vitro* the cytotoxic effects of tipifarnib in combination with three agents of small molecular weight – rapamycin (an inhibitor of the mammalian target of rapamycin [mTOR]), LY294002 (an inhibitor of PI3-kinase), and U0126 (an inhibitor of MEK1/2) – in efforts to identify effective therapeutic combinations. We found that the combination of tipifarnib and rapamycin, which has also been shown to inhibit the growth of leukemia cells [14,15], had a synergistic inhibitory effect on the growth of BCR/ABL-negative leukemia cell lines as well as BCR/ABL-positive cell lines. Importantly, this combination also showed

* Corresponding author. Tel.: +81 285 58 7353; fax: +81 285 44 5258.
E-mail address: t-nagai@jichi.ac.jp (T. Nagai).

0145-2126/$ – see front matter © 2010 Elsevier Ltd. All rights reserved.
doi:10.1016/j.leukres.2009.12.011

synergistic antiproliferative effects in tipifarnib-resistant K562/RR cells. These findings suggest that the combination of tipifarnib and rapamycin is a potential therapy for various types of leukemia and is also effective for overcoming resistance to tipifarnib.

2. Materials and methods

2.1. Cell lines

K562, KCL22, and KU812 are BCR/ABL-positive cell lines established from the peripheral blood of patients with chronic myelogenous leukemia (CML) in blast crisis [16–18]. K562/RR is a tipifarnib-resistant cell line cloned from K562 in our laboratory [19]. U937 and THP-1 are BCR/ABL-negative human myeloid leukemia cell lines [20,21]. These cells were grown in RPMI-1640 medium supplemented with 10% fetal bovine serum and split every 4 days. Cell numbers were counted using a Cell Counting Kit-8 (Wako Pure Chemical Industries, Ltd., Osaka, Japan) in accordance with the manufacturer's instructions.

2.2. Reagents

Tipifarnib was kindly provided by Johnson & Johnson Pharmaceutical Research & Development (Titusville, NJ). Rapamycin, LY294002, and U0126 were purchased from Sigma Chemical Co. (St. Louis, MO).

2.3. Cytotoxic effects of combinations of tipifarnib and other small molecules

Cells were incubated with various concentrations of agents for 4 days, and cell numbers were then counted using a Cell Counting Kit-8. The cytotoxic effects of the combinations of tipifarnib and other compounds of small molecular weight were

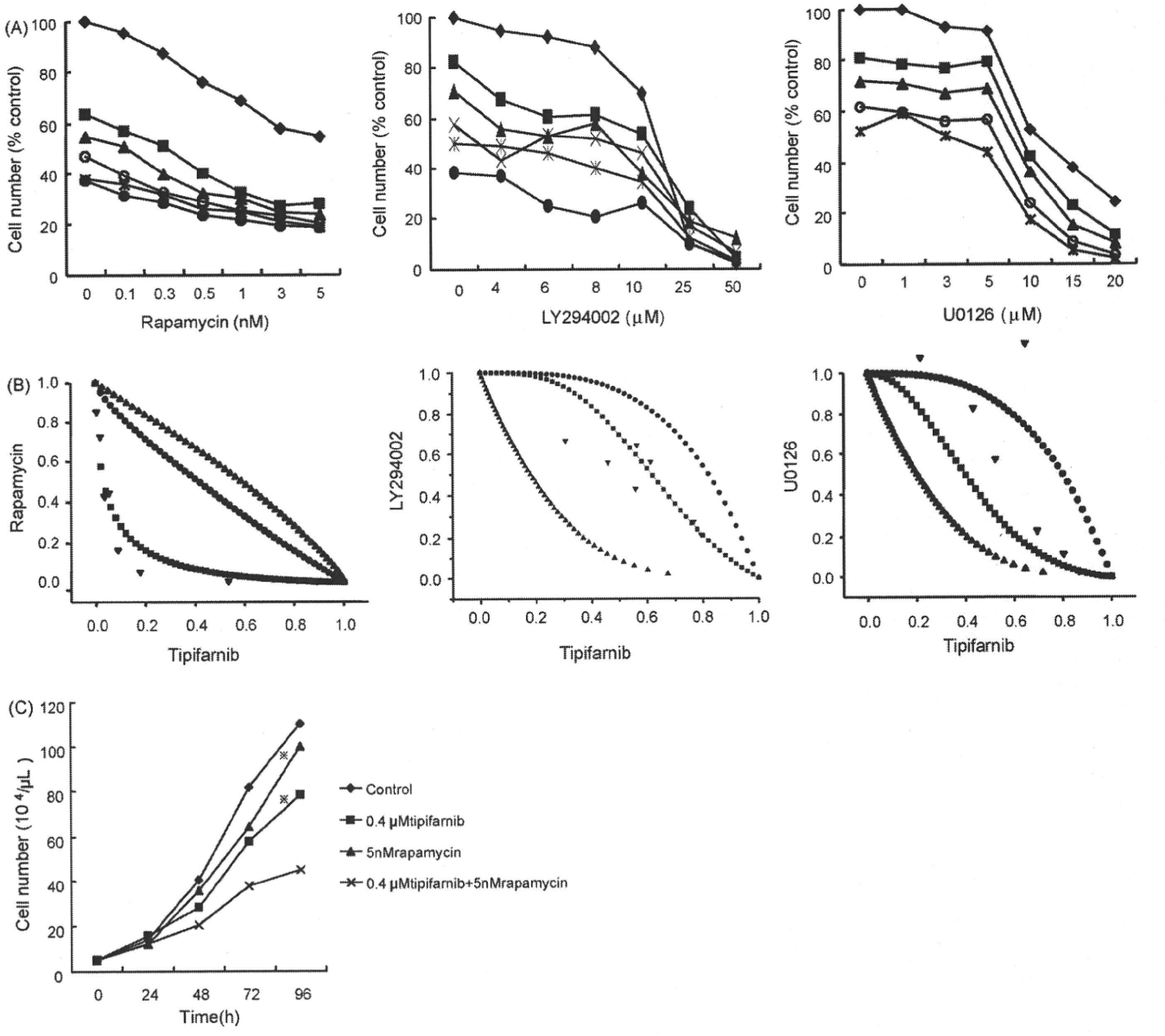

Fig. 1. Inhibitory effects of tipifarnib in combination with other agents on growth of K562 cells. (A) Dose–response curves of tipifarnib in combination with rapamycin, LY294002, and U0126. Cells were cultured with various concentrations of tipifarnib for 4 days in the presence of the indicated concentrations of each agent, and the number of viable cells was then counted with a Cell Counting Kit-8. The concentrations of tipifarnib were as follows: 0 μM (♦); 0.2 μM (■); 0.4 μM (▲); 0.6 μM (○); 0.8 μM (×); 1.0 μM (●) for rapamycin; 0 μM (♦); 0.2 μM (■); 0.4 μM (▲); 0.5 μM (○); 0.6 μM (×); 1.0 μM (●) for LY294002; and 0 μM (♦); 0.05 μM (■); 0.10 μM (▲); 0.25 μM (○); 0.50 μM (×) for U0126. (B) Steel and Peckham isobologram analyses of the combinations of tipifarnib with rapamycin, LY294002, and U0126 in K562 cells were performed as described in Section 2. The combination of tipifarnib and rapamycin showed a synergistic effect, whereas other combinations showed only additive effects. (C) K562 cells were incubated with 0.4 μM tipifarnib, 5 nM rapamycin, or with a combination of 0.4 μM tipifarnib and 5 nM rapamycin. The number of viable cells was counted at each time point using trypan blue staining. Each point represents the mean value of three independent experiments. Statistical analysis was carried out using Scheffe's test for comparison of the data between cells treated with a combination of tipifarnib and rapamycin and cells treated with tipifarnib alone, and between cells treated with a combination of tipifarnib and rapamycin and cells treated with rapamycin alone (Asterisk denotes $P<0.05$).

evaluated by Steel and Peckham isobolograms as described previously [22]. In this analysis, when the points lie outside the left margin of the envelope, the combination treatment is considered to have a synergistic inhibitory effect on cell growth. If the points lie within the envelope, the combination treatment is considered to have an additive effect.

2.4. Western blot analysis

Nuclear extracts were prepared from 1×10^7 cells according to a method described previously [23]. Then, 10 μg of nuclear extract was separated electrophoretically using a 10% polyacrylamide gel. Immunoblotting and detection by enhanced chemiluminescence were performed as described previously [23]. A mouse monoclonal antibody against glyceraldehyde-3-phosphate dehydrogenase, which was used as an internal control, was purchased from Chemicon International (Temecula, CA). Rabbit polyclonal antibodies against caspase-3, cleaved caspase-3, caspase-9, cleaved caspase-9, PARP, cleaved PARP, cytochrome c, phospho-cdc2, Chk2, phospho-Chk2, Mcl-1, BCR, phospho-BCR, phospho-CrkL, p44/42 (ERK1/2) MAP kinase, phospho-p44/42 (ERK1/2) MAP kinase, JNK, phospho-JNK, STAT5, and phospho-STAT5 as well as mouse monoclonal antibodies against CDK4, cyclin D1, and cyclin D3 were purchased from Cell Signaling Technology (Beverly, MA). Mouse anti-$p27^{KIP1}$ monoclonal antibody was purchased from BD Biosciences (San Jose, CA).

2.5. Flow cytometry

Flow cytometric analysis was performed as described previously [19]. Briefly, the cells were incubated with propidium iodide for 30 min and analyzed by flow cytometry with a FACScan/CellFIT system (Becton Dickinson, San Jose, CA).

3. Results

3.1. Combined treatment of K562 cells with tipifarnib and rapamycin resulted in synergistic inhibition of cell growth

To examine the cytotoxic effects of tipifarnib in combination with other agents of small molecular weight, including rapamycin, LY294002, and U0126, Steel and Peckham isobologram analysis was performed using K562 cells. The IC_{50} values of tipifarnib, rapamycin, LY294002, and U0126 against K562 cells are 0.4 μM, 5 nM, 12 μM, and 13 μM, respectively. The dose–response curves for tipifarnib in combination with those small molecules are shown in Fig. 1A. Isobolograms were then created on the basis of the results of the dose–response curves. As shown in Fig. 1B, all points for a combination of tipifarnib and rapamycin lay outside the left margin of the envelope, indicating a clear synergistic inhibitory effect on the growth of the cells. Consistent with these results, combined treatment of K562 cells with the IC_{50} concentrations of tipifarnib (0.4 μM) and rapamycin (5 nM) resulted in more significant inhibition of growth than did either tipifarnib or rapamycin alone (Fig. 1C). In contrast, combinations of tipifarnib and LY294002 or tipifarnib and U0126 showed no synergistic inhibition but had an additive effect on the growth of the cells (Fig. 1B). These results indicate that although combinations of tipifarnib and all three other small molecules enhanced the cytotoxic effect, rapamycin was the most effective partner of tipifarnib for combination therapy.

3.2. Induction of apoptosis and cell-cycle blockage in K562 cells by the combination of tipifarnib and rapamycin

We next performed flow cytometry analysis to clarify whether induction of apoptosis and blockage of the cell cycle are involved in the synergistic inhibition of cell growth (Fig. 2). When tipifarnib was added to K562 cells as a single agent, the percentage of sub-G1 cells was increased, whereas that of G0/G1 cells was unchanged. In contrast, rapamycin alone increased the percentage of G0/G1 cells, which is consistent with the results of a previous study showing that rapamycin induces G0/G1 arrest [14], with a decrease in the percentage of sub-G1 cells. Combined treatment of K562 cells with tipifarnib and rapamycin also resulted in an increase in the percentage of G0/G1 cells at 24 h ($P = 0.028$). Furthermore, the combination showed a tendency toward induction of sub-G1 cells, although this effect was not significant ($P = 0.197$ and 0.226 at 24 h and 48 h, respectively). Therefore, it is likely that the synergistic inhibition

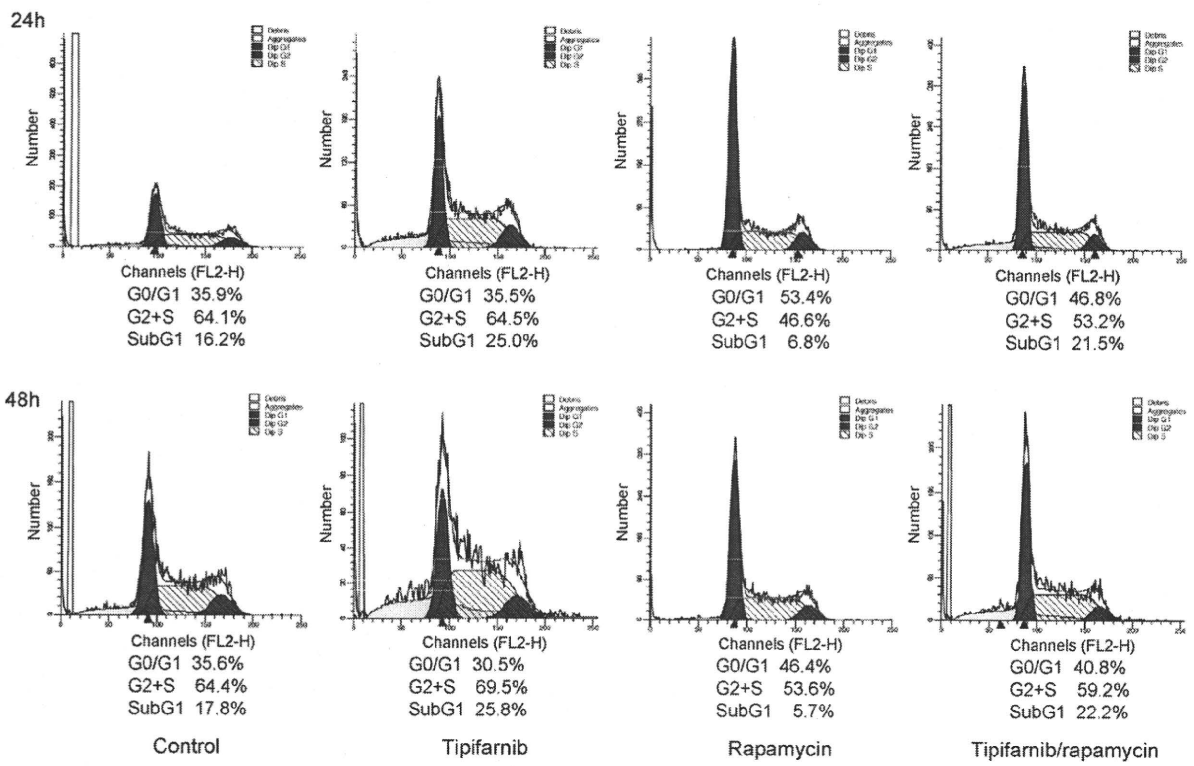

Fig. 2. Effect of the combination of tipifarnib and rapamycin on the induction of apoptosis and cell-cycle blockage. After cells were incubated for 24 and 48 h with tipifarnib, rapamycin, or a combination of tipifarnib and rapamycin, the cells were harvested and incubated with propidium iodide for 30 min and analyzed by flow cytometry with a FACScan/CellFIT system (Becton Dickinson, San Jose, CA). The results shown are representative of three independent experiments.

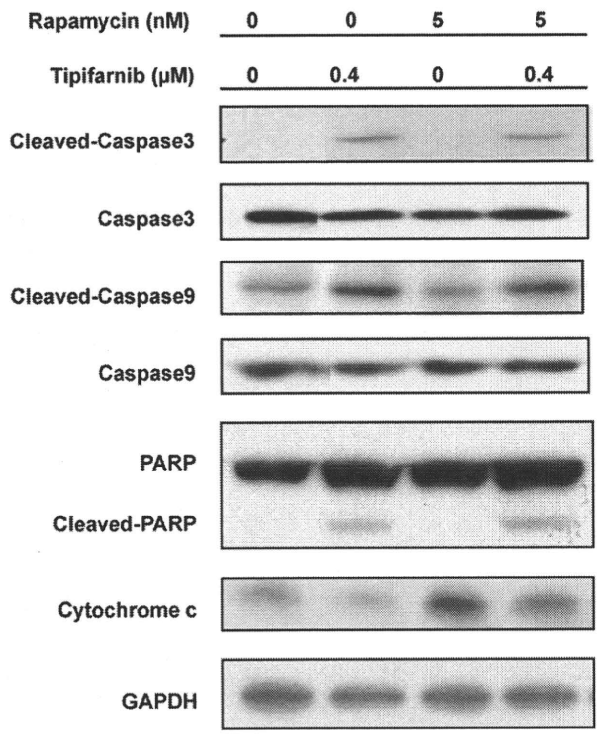

Fig. 3. Effect of the combination of tipifarnib and rapamycin on the levels of molecules related to apoptosis. Cells were treated with tipifarnib, rapamycin, or a combination of tipifarnib and rapamycin for 24 h. Total cell lysates were prepared and subjected to Western blot analysis using antibodies against cleaved caspase-3, caspase-3, cleaved caspase-9, caspase-9, cleaved PARP, and PARP. Mitochondrial lysates were prepared and subjected to Western blot analysis using anti-cytochrome c antibody. The expression of glyceraldehyde-3-phosphate dehydrogenase (GAPDH) is shown as an internal control.

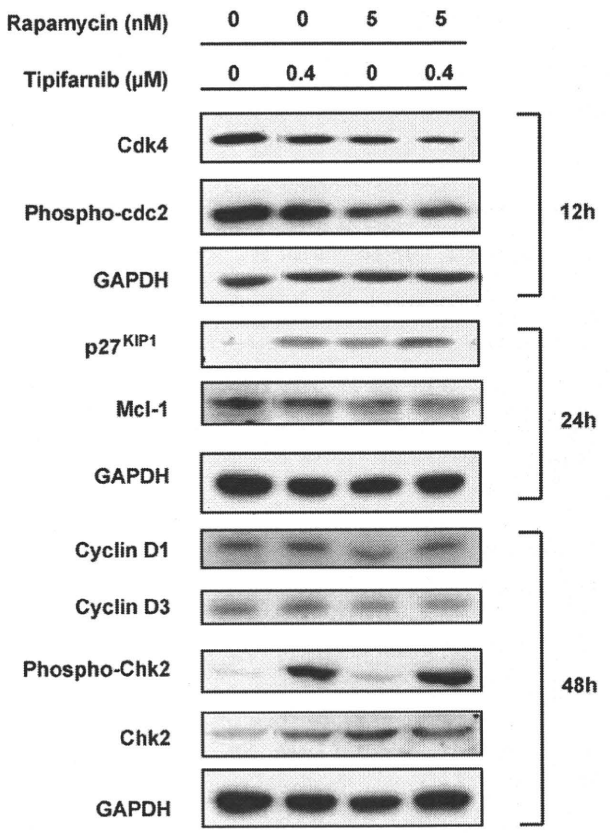

Fig. 4. Effect of the combination of tipifarnib and rapamycin on the levels of molecules related to the cell cycle. Cells were cultured with tipifarnib, rapamycin, or a combination of tipifarnib and rapamycin for the indicated times. Total cell lysates were prepared and subjected to Western blot analysis using indicated antibodies. The expression of GAPDH is shown as an internal control.

of growth mediated by the combination involved both apoptosis and blockage of the cell cycle.

3.3. *Effect of the combination of tipifarnib and rapamycin on the levels of molecules related to apoptosis*

We then examined the effect of the combination of tipifarnib and rapamycin on the levels of molecules related to apoptosis. The combination induced cleaved caspase-3, cleaved caspase-9, and cleaved PARP to levels similar to those induced when tipifarnib was added as a single agent (Fig. 3). In contrast, rapamycin alone had no effect on the levels of these molecules. The level of cytochrome c in a mitochondrial fraction was somewhat increased by rapamycin alone but was decreased when tipifarnib was added as a single agent or in combination with rapamycin. These results suggest that either tipifarnib alone or the combination of tipifarnib and rapamycin induced apoptosis by the release of cytochrome c from mitochondria with subsequent activation of the caspase pathway.

3.4. *Effect of the combination of tipifarnib and rapamycin on the levels of molecules related to the cell cycle*

The combination of tipifarnib and rapamycin also influenced the levels of molecules involved in the regulation of the cell cycle. When rapamycin was added to K562 cells as a single agent, a notable increase in the level of p27 and slight reductions in the levels of cdk4, phospho-cdc2, Mcl-1, and cyclin D3 were observed (Fig. 4). Tipifarnib alone also increased the level of p27, but it reduced the level of cdk4 to a lesser extent and had no effect on the levels of phospho-cdc2, Mcl-1, and cyclin D3. Importantly, the combination of tipifarnib and rapamycin increased the level of p27 and decreased the level of cdk4 to greater extents than did tipifarnib or rapamycin alone (Fig. 4). Taken together, these results suggest that tipifarnib contributed primarily to the induction of apoptosis and influenced cell-cycle regulation to a lesser extent, whereas rapamycin was mainly involved in blockage of the cell cycle in the cells treated with the combination. In this case, neither reagent reduced the effect of the other. Interestingly, the level of phospho-Chk2 was significantly increased by tipifarnib alone or in the combination, whereas it was not changed with rapamycin alone. These results suggest that the blockage of the cell cycle induced by rapamycin was not mediated by activation of Chk2 (Fig. 4).

3.5. *Combination of tipifarnib and rapamycin inhibited STAT5, JNK, and ERK1/2 activities*

We then examined the effect of the combination of tipifarnib and rapamycin on cellular signaling pathways. As shown in Fig. 5, tipifarnib alone and tipifarnib in combination with rapamycin markedly reduced the level of phospho-STAT5. The level of phospho-STAT5 was also decreased by treatment with rapamycin at 6 h, but this effect was modest and transient. In contrast, rapamycin induced a higher level of phospho-JNK/SAPK at 12 h. Therefore, suppression of STAT5 activity might be involved in the tipifarnib-mediated induction of apoptosis, whereas activation of the JNK-SAPK pathway might play a role in the blockage of the cell cycle induced by rapamycin.

Interestingly, treatment of the cells with a combination of tipifarnib and rapamycin resulted in pronounced reduction of the

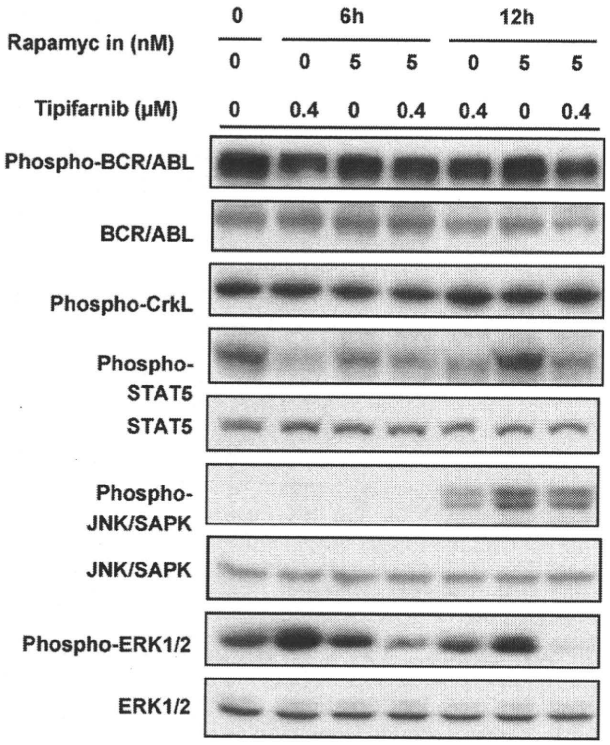

Fig. 5. Effect of the combination of tipifarnib and rapamycin on the levels of molecules related to signaling pathways. Cells were treated with tipifarnib, rapamycin, or a combination of tipifarnib and rapamycin and harvested at each time point. Total cell lysates were prepared and subjected to Western blot analysis using the indicated antibodies.

phospho-ERK1/2 level from 6 h to 12 h after the start of treatment, whereas the level of phospho-ERK1/2 was increased transiently and slightly by tipifarnib alone and was not changed when rapamycin was added as a single agent. Therefore, it is possible that a potent suppression of ERK1/2 activity is involved in the synergy displayed by the combination. In contrast, the combination had no effect on the levels of phospho-BCR/ABL and phospho-CrkL, which is a substrate of BCR/ABL, suggesting that the combination had no effect on BCR/ABL activity.

3.6. Combination of tipifarnib and rapamycin synergistically inhibited growth of various types of leukemia cells

Drug resistance is a serious problem for patients being treated with agents of small molecular weight such as tipifarnib. It was, therefore, important to reveal whether the combination treatment also effectively inhibited the growth of tipifarnib-resistant cells. To address this question, we examined the effect of the combination on growth of the tipifarnib-resistant cell line K562/RR, which was recently cloned from K562 in our laboratory [19], by isobologram analysis. Combined treatment of K562/RR cells with tipifarnib and rapamycin resulted in synergistic inhibition of growth with the accumulation of both G0/G1 phase and sub-G1 phase cells (Fig. 6A, data not shown). In contrast, tipifarnib in combination with LY294002 or U0126 merely additively inhibited growth of K562/RR cells (Fig. 6A). We further examined the cytotoxic effect of the combination in the other human BCR/ABL-positive leukemia cell lines KCL22 and KU812 as well as in the human BCR/ABL-negative leukemia cell lines U937 and THP-1. Fig. 6B shows that the combination of tipifarnib and rapamycin also synergistically inhibited the growth of all cell lines examined. These results suggest that the effect of the combination of tipifarnib and rapamycin is not restricted to K562 cells but that this combination is effective for various types of leukemia cells, including tipifarnib-resistant cells, regardless of the presence or absence of BCR/ABL protein.

3.7. Tipifarnib and rapamycin effectively inhibited the growth of leukemia cells from a patient with acute myeloid leukemia

To clarify whether the combination effectively inhibits growth of primary leukemia cells, we next examined the cytotoxic effect of combined treatment using primary leukemia cells from the peripheral blood of a patient with acute myeloid leukemia. Written informed consent for the examination was obtained from the patient. As shown in Fig. 7, the combination of tipifarnib and rapamycin enhanced the inhibition of growth in the primary

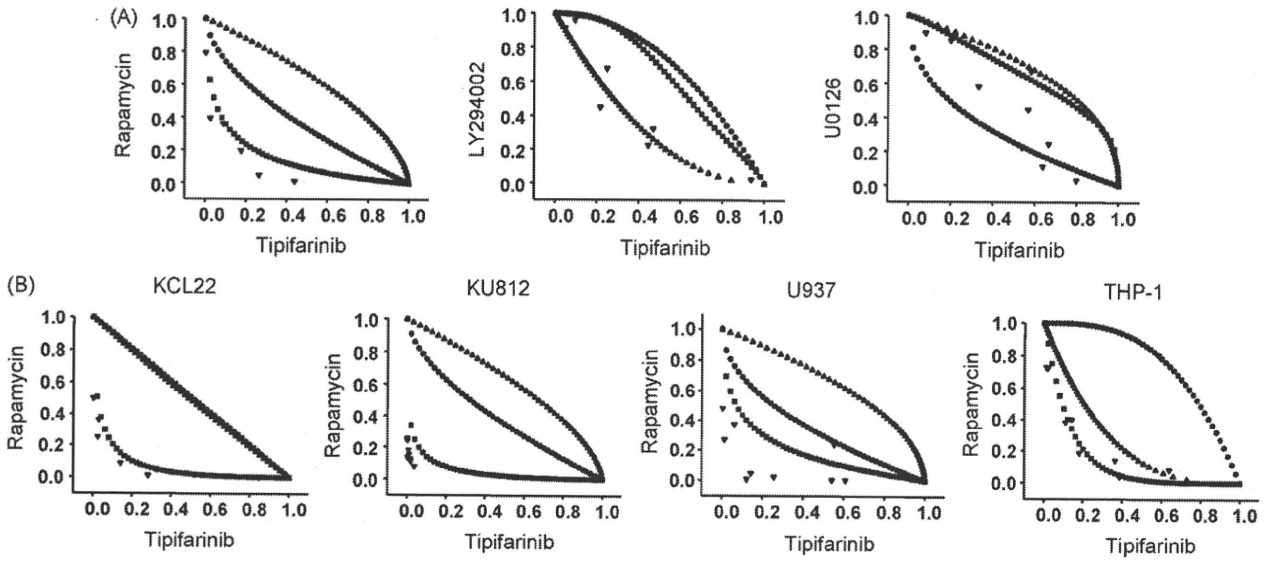

Fig. 6. Cytotoxic effect of tipifarnib in combination with rapamycin in various leukemia cell lines. (A) Steel and Peckham isobologram analyses of the combinations of tipifarnib with rapamycin, LY294002, and U0126 in tipifarnib-resistant K562/RR cells were performed as described in Section 2. The combination of tipifarnib and rapamycin showed a synergistic effect, whereas other combinations showed only an additive effect. (B) Steel and Peckham isobologram analyses of the effects of the combination of tipifarnib and rapamycin in BCR/ABL-positive KCL22 and KU812 cells and BCR/ABL-negative U937 and THP-1 cells were performed as described in Section 2. Most points lie within the area representing synergistic effects.

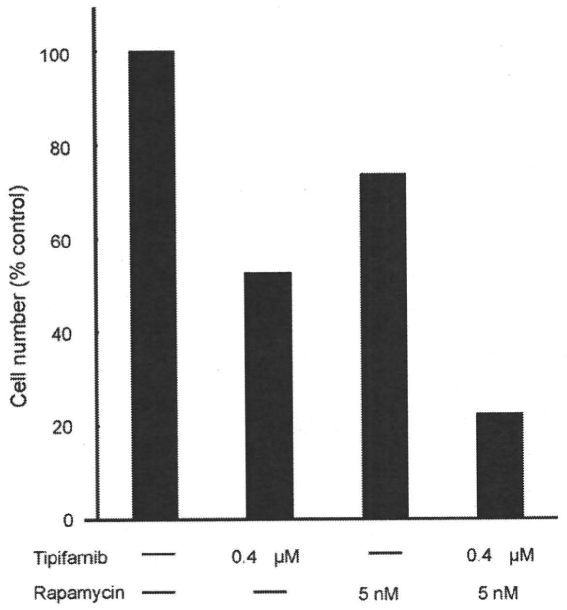

Fig. 7. Effect of the combination of tipifarnib and rapamycin on the inhibition of growth of primary leukemia cells. Primary leukemia cells from the peripheral blood of a patient with acute myeloid leukemia were incubated with 0.4 μM tipifarnib, 5 nM rapamycin, or with a combination of 0.4 μM tipifarnib and 5 nM rapamycin for 5 days. The number of viable cells was counted by trypan blue staining. Percentage of cell number is shown.

leukemia cells, suggesting that the combination is also effective against primary leukemia cells.

4. Discussion

Development of therapeutic strategies using small molecular weight agents is very attractive for the treatment of hematologic malignancies. However, mono-therapy with these agents occasionally shows limited clinical efficacy. One possible approach for making good use of these agents is the establishment of effective combination therapies. For this purpose, we examined the effect of the farnesyltransferase inhibitor tipifarnib in combination with other therapeutic agents of small molecular weight on the growth of leukemia cells.

It has been shown that Steel and Peckham isobologram analysis provides stringent and reliable results for the cytotoxic effects of combination treatments [22]. Using this analysis, we found that the combination of tipifarnib and rapamycin synergistically inhibited the growth of leukemia cells. Notably, this synergistic effect was also observed in tipifarnib-resistant K562/RR cells, which are likely to acquire resistance by farnesyltransferase activity-independent mechanisms, such as continuous activation of signaling pathways [19]. Because acquisition of drug resistance is frequently found in patients treated with small molecules, it was important to show the potential to overcome resistance to tipifarnib with this combination. Acquisition of resistance to tipifarnib might also be caused by other mechanisms, such as inability to block farnesylation. Indeed, it has been shown that insertion of mutations in the farnesyltransferase β gene resulted in the acquisition of resistance to tipifarnib [24], although patients whose disease is resistant to tipifarinib because of mutations in the farnesyltransferase gene have not yet been described. Recently, Raponi et al. [25] found by analysis of gene expression profiles from patients treated with tipifarnib that a low ratio of the expression level of RASGRP1/APTX predicts a poor response to tipifarnib. It is therefore of interest to clarify whether the combination of tipifarnib and rapamycin is also effective in AML cells for which such a poor response is predicted. Unlike the combination with rapamycin, combinations of tipifarnib with other agents, including LY294002 and U0126, had additive inhibitory effects on growth, suggesting that rapamycin is a particularly good combination partner for tipifarnib.

It is likely that tipifarnib and rapamycin contributed to the inhibition of leukemia cell growth in different manners. Our results demonstrate that tipifarnib was mainly involved in the induction of apoptosis, which is consistent with the results of previous studies showing that tipifarnib induces apoptosis in hematologic malignant cells [26,27]. In contrast, rapamycin was involved in blockage of the cell cycle and slightly blocked spontaneous apoptosis. These results are consistent with the results of a previous study showing that rapamycin inhibits the growth of acute myeloid leukemia cells by blocking the cell cycle in G0/G1 phase [14].

Clarification of the molecular mechanisms of the effects of each agent is of great interest. Administration of tipifarnib alone, rapamycin alone, and co-administration of these agents all increased the level of phospho-JNK (Fig. 5). It is, therefore, possible that up-regulation of JNK activity is involved in the induction of cell-cycle blockage in K562 cells treated with rapamycin or tipifarnib. Because rapamycin has been shown to reduce JNK activity in several cell types [28–30], it is likely that rapamycin has distinct effects on JNK signaling, depending on the type of cell. In support of this hypothesis, there has been a study demonstrating that rapamycin potentiates the cytotoxicity of UCN-01, which is a Chk1 and protein kinase C inhibitor, accompanied by phosphorylation of JNK [31]. In contrast, the level of phospho-STAT5 was significantly reduced by tipifarnib alone or by tipifarnib in combination with rapamycin (Fig. 5). Although the direct target proteins through which tipifarnib mediates tumor suppression remain to be identified, our results suggest that tipifarnib affects the activities of molecules related to cellular signaling, including STAT5 and JNK.

We hypothesize that co-administration of tipifarnib and rapamycin alters a network of cellular signaling pathways. In support of this hypothesis, the combination markedly reduced the level of phospho-ERK1/2 (Fig. 5). The fact that enforced expression of MEK1, an upstream serine-threonine kinase of ERK1/2, in KCL22 cells resulted in no abrogation of the combination-mediated synergistic inhibitory effect on growth (data not shown) and the fact that the combination of tipifarnib and the MEK1/2 inhibitor U0126 showed no synergistic effect (Fig. 1) suggest that ERK1/2 activity was not the only target involved in the synergy induced by the combination. However, it is possible that alteration of the signaling pathway network mediated by the combination is required for developing the synergy. On the other hand, tipifarnib did not enhance the rapamycin-mediated inhibition of phosphorylation of 4EBP1 and p70 S6, which are downstream molecules of the mTOR pathway (data not shown). Although it has been reported that the farnesyltransferase inhibitor lonafarnib inhibits mTOR signaling [32], our results suggest that tipifarnib had no effect on the inhibition of mTOR function mediated by rapamycin and that mTOR activity was not related to the synergistic effect of tipifarnib and rapamycin.

In conclusion, the findings in this study demonstrated that the combinations of tipifarnib and rapamycin, LY294002, or U0126 have advantages for the treatment of leukemia. In particular, the combination of tipifarnib and rapamycin synergistically inhibited the growth of leukemia cells, including tipifarnib-resistant cells, by induction of apoptosis as well as blockage of the cell cycle. These findings indicate the potential clinical application of combination therapies with tipifarnib.

Conflict of interest

None

Acknowledgements

This work was supported in part by Grants-in-Aid from the Ministry of Education, Culture, Sports, Science, and Technology, Japan, and the Japan Leukaemia Research Fund (to T.N.). We wish to thank Ms. E. Yamakawa for her help in preparation of the manuscript.

References

[1] Chen GQ, Wang LS, Wu YL, Yu Y. Leukemia, an effective model for chemical biology and target therapy. Acta Pharmacol Sin 2007;28:1316–24.
[2] Jabbour E, Cortes J, O'Brien S, Giles F, Kantarjian H. New targeted therapies for chronic myelogenous leukemia: opportunities to overcome imatinib resistance. Semin Hematol 2007;44(1 Suppl. 1):S25–31.
[3] Fröhling S, Scholl C, Gilliland DG, Levine RL. Genetics of myeloid malignancies: pathogenetic and clinical implications. J Clin Oncol 2005;23:6285–95.
[4] Gotlib J. Farnesyltransferase inhibitor therapy in acute myelogenous leukemia. Curr Hematol Rep 2005;4:77–84.
[5] Feldman EJ. Farnesyltransferase inhibitors in myelodysplastic syndrome. Curr Hematol Rep 2005;4:186–90.
[6] Karp JE, Lancet JE, Kaufmann SH, End DW, Wright JJ, Bol K, et al. Clinical and biologic activity of the farnesyltransferase inhibitor R115777 in adults with refractory and relapsed acute leukemias: a phase 1 clinical–laboratory correlative trial. Blood 2001;97:3361–9.
[7] Lancet JE, Gojo I, Gotlib J, Feldman EJ, Greer J, Liesveld JL, et al. A phase 2 study of the farnesyltransferase inhibitor tipifarnib in poor-risk and elderly patients with previously untreated acute myelogenous leukemia. Blood 2007;109:1387–94.
[8] Harousseau JL, Lancet JE, Reiffers J, Lowenberg B, Thomas X, Huguet F, et al. Farnesyltransferase Inhibition Global Human Trials (FIGHT) Acute Myeloid Leukemia Study Group. A phase 2 study of the oral farnesyltransferase inhibitor tipifarnib in patients with refractory or relapsed acute myeloid leukemia. Blood 2007;109:5151–6.
[9] Harousseau JL, Martinelli G, Jedrzejczak WW, Brandwein JM, Bordessoule D, Masszi T, et al. A randomized phase 3 study of tipifarnib compared to best supportive care, including hydroxyurea, in the treatment of newly diagnosed acute myeloid leukemia (AML) in patients 70 years or older. Blood 2009 Jun 11 [Epub ahead of print].
[10] Cortes J, Albitar M, Thomas D, Giles F, Kurzrock R, Thibault A, et al. Efficacy of the farnesyl transferase inhibitor R115777 in chronic myeloid leukemia and other hematologic malignancies. Blood 2003;101:1692–7.
[11] Alsina M, Fonseca R, Wilson EF, Belle AN, Gerbino E, Price-Troska T, et al. Farnesyltransferase inhibitor tipifarnib is well tolerated, induces stabilization of disease, and inhibits farnesylation and oncogenic/tumor survival pathways in patients with advanced multiple myeloma. Blood 2004;103:3271–7.
[12] Miyoshi T, Nagai T, Ohmine K, Nakamura M, Kano Y, Muroi K, et al. Relative importance of apoptosis and cell cycle blockage in the synergistic effect of combined R115777 and imatinib treatment in BCR/ABL-positive cell lines. Biochem Pharmacol 2005;69:1585–94.
[13] Karp JE, Flatten K, Feldman EJ, Greer JM, Loegering DA, Ricklis RM, et al. Active oral regimen for elderly adults with newly diagnosed acute myelogenous leukemia: a preclinical and phase I trial of the farnesyltransferase inhibitor tipifarnib (R115777, Zarnestra) combined with etoposide. Blood 2009;113:4841–52.
[14] Récher C, Beyne-Rauzy O, Demur C, Chicanne G, Dos Santos C, Mas VM, et al. Antileukemic activity of rapamycin in acute myeloid leukemia. Blood 2005;105:2527–34.
[15] Récher C, Dos Santos C, Demur C, Payrastre B. mTOR, a new therapeutic target in acute myeloid leukemia. Cell Cycle 2005;4:1540–9.
[16] Lozzio CB, Lozzio BB. Human chronic myelogenous leukemia cell-line with positive Philadelphia chromosome. Blood 1975;45:321–34.
[17] Kubonishi I, Miyoshi I. Establishment of a Ph1 chromosome-positive cell line from chronic myelogenous leukemia in blast crisis. Int J Cell Cloning 1983;1:105–17.
[18] Kishi K. A new leukemia cell line with Philadelphia chromosome characterized as basophil precursors. Leuk Res 1985;9:381–90.
[19] Miyoshi T, Nagai T, Kikuchi S, Ohmine K, Nakamura M, Hanafusa T, et al. Cloning and characterization of a human BCR/ABL-positive cell line, K562/RR, resistant to the farnesyltransferase inhibition by tipifarnib. Exp Hematol 2007;35:1358–65.
[20] Collins SJ, Gallo RC, Gallagher RE. Continuous growth and differentiation of human myeloid leukaemic cells in suspension culture. Nature 1977;270:347–9.
[21] Sundstrom C, Nilsson K. Establishment and characterization of a human histiocytic lymphoma cell line (U-937). Int J Cancer 1976;17:565–77.
[22] Kano Y, Akutsu M, Tsunoda S, Mano H, Sato Y, Honma Y, et al. In vitro cytotoxic effects of a tyrosine kinase inhibitor STI571 in combination with commonly used antileukemic agents. Blood 2001;97:1999–2007.
[23] Nagai T, Igarashi K, Akasaka J, Furuyama K, Fujita H, Hayashi N, et al. Regulation of NF-E2 activity in erythroleukemia cell differentiation. J Biol Chem 1998;27:5358–65.
[24] Del Villar K, Urano J, Guo L, Tamanoi F. A mutant form of human protein farnesyltransferase exhibits increased resistance to farnesyltransferase inhibitors. J Biol Chem 1999;274:27010–7.
[25] Raponi M, Lancet JE, Fan H, Dossey L, Lee G, Gojo I, et al. A 2-gene classifier for predicting response to the farnesyltransferase inhibitor tipifarnib in acute myeloid leukemia. Blood 2008;111:2589–96.
[26] Korycka A, Smolewski P, Robak T. The influence of farnesyl protein transferase inhibitor R115777 (Zarnestra) alone and in combination with purine nucleoside analogs on acute myeloid leukemia progenitors in vitro. Eur J Haematol 2004;73:418–26.
[27] Medeiros BC, Landau HJ, Morrow M, Lockerbie RO, Pitts T, Eckhardt SG. The farnesyl transferase inhibitor, tipifarnib, is a potent inhibitor of the MDR1 gene product, P-glycoprotein, and demonstrates significant cytotoxic synergism against human leukemia cell lines. Leukemia 2007;21:739–46.
[28] Ishizuka T, Sakata N, Johnson GL, Gelfand EW, Terada N. Rapamycin potentiates dexamethasone-induced apoptosis and inhibits JNK activity in lymphoblastoid cells. Biochem Biophys Res Commun 1997;230:386–91.
[29] Morley SJ, McKendrick L. Involvement of stress-activated protein kinase and p38/RK mitogen-activated protein kinase signaling pathways in the enhanced phosphorylation of initiation factor 4E in NIH 3T3 cells. J Biol Chem 1997;272:17887–93.
[30] Miller AL, Garza AS, Johnson BH, Thompson EB. Pathway interactions between MAPKs, mTOR, PKA, and the glucocorticoid receptor in lymphoid cells. Cancer Cell Int 2007;7:3.
[31] Hahn M, Li W, Yu C, Rahmani M, Dent P, Grant S. Rapamycin and UCN-01 synergistically induce apoptosis in human leukemia cells through a process that is regulated by the Raf-1/MEK/ERK, Akt, and JNK signal transduction pathways. Mol Cancer Ther 2005;4:457–70.
[32] Basso AD, Mirza A, Liu G, Long BJ, Bishop WR, Kirschmeier P. The farnesyl transferase inhibitor (FTI) SCH66336 (lonafarnib) inhibits Rheb farnesylation and mTOR signaling. Role in FTI enhancement of taxane and tamoxifen anti-tumor activity. J Biol Chem 2005;280:31101–8.

Bone Marrow Transplantation (2010) 45, 723–729

www.nature.com/bmt

ORIGINAL ARTICLE

IL-21 is critical for GVHD in a mouse model

A Meguro[1], K Ozaki[1], I Oh[1], K Hatanaka[1], H Matsu[1], R Tatara[1], K Sato[1], WJ Leonard[2] and K Ozawa[1]

[1]*Division of Hematology, Department of Medicine, Jichi Medical University Tochigi, Tochigi, Japan and* [2]*Laboratory of Molecular Immunology, National Heart, Lung and Blood Institute, National Institutes of Health, Bethesda, MD, USA*

Immunological effects of IL-21 on T, B and natural killer (NK) cells have been reported, but the role of IL-21 in GVHD remains obscure. Here, we demonstrate that morbidity and mortality of GVHD was significantly reduced after BMT with splenocytes from IL-21R$^{-/-}$ mice compared with those from wild type mice. To further confirm our observation, we generated a decoy receptor for IL-21. GVHD was again less severe in mice receiving BM cells transduced with the IL-21 decoy receptor than control mice These results suggest that IL-21 critically regulates GVHD, and that blockade of the IL-21 signal may represent a novel strategy for the prophylaxis for GVHD.
Bone Marrow Transplantation (2010) **45,** 723–729; doi:10.1038/bmt.2009.223; published online 31 August 2009
Keywords: GVHD; IL-21; hematopoietic SCT

Introduction

Interleukin (IL)-21 is a member of the common cytokine receptor gamma chain (γ_c) family that also includes IL-2, IL-4, IL-7, IL-9 and IL-15. The receptors for each of these cytokines are composed of more specific chain(s) and a γ_c chain.[1,2] The lack of functional γ_c causes X-linked SCID disease (X-SCID) in humans,[3] which is characterized by a reduced number of T cells and natural killer (NK) cells, and a normal number but non-functional B cells. The phenotypes of IL-7 and IL-15 knockout (KO) mice suggest that the reduced number of T and NK cells is because of the lack of IL-7 and IL-15 signaling, respectively.[4,5] We previously proposed that the non-functionality of B cells might be attributed to the lack of both IL-4 and IL-21, based on the observation that IL-4 and IL-21R double KO mice exhibit a B-cell phenotype similar to that found in X-linked SCID disease.[6] The switch from IgM to IgG was impaired but still present in IL-21R$^{-/-}$ mice.[6]

IL-21 was cloned as a co-stimulatory cytokine for T-cell proliferation and NK-cell expansion *in vitro*.[7] IL-21 is primarily produced by CD4 T cells,[7] and the receptor is primarily expressed on T, B and NK cells.[7,8] It has been reported that IL-21 suppresses the function of DCs[9] and increases the number of hematopoietic progenitor cells.[10] IL-21 has been shown to have critical roles in Ig production.[6] IL-21 is not required, but promotes Th17 differentiation in the presence of transforming growth factor (TGF)-β,[11–13] whereas reports have differed regarding its contributions to Th1- and Th2-differentiation.[6,14–17] Evidence for a relationship between IL-21 and autoimmune disease has been accumulating. For example, overexpression of IL-21 induces inflammation, and in the BXSB.6-Yaa$^+$/J mouse, a model of systemic lupus erythematosus, affected mice have high levels of IL-21,[18] whereas IL-21R$^{-/-}$ BXSB.6-Yaa$^+$/J mice no longer develop systemic lupus erythematosus.[19] In addition, IL-21R$^{-/-}$ NOD mice are resistant to the development of diabetes mellitus.[20,21]

Graft-versus-host disease is a serious complication after hematopoietic SCT.[22] Severe GVHD is difficult to treat because of refractory characteristics and infectious complications resulting from immunosuppressive treatment.

Here, we have investigated the function of IL-21 in GVHD and demonstrate that IL-21 is critical for GVHD, and that blockade of the IL-21 signal could lead to a treatment or prophylaxis for GVHD.

Methods

Mice

Interleukin-21R$^{-/-}$ (KO) mice were generated previously.[6] Balb/c mice were purchased from Clea Japan (Tokyo, Japan). *Perforin*-deficient mice and FasL deficient (*gld*/*gld*) mice were purchased from Taconic (Hudson, NY, USA) and Japan SLC (Shizuoka, Japan), respectively. All mice were housed in our mouse facility, which is regulated by an intramural small animal committee, and were treated in accordance with the guidelines of Jichi Medical University.

Mouse models of GVHD and GVL

Clinical symptoms of GVHD were scored as previously reported.[23]

GVHD group 1 (*WT-BM and KO-SP vs WT-BM and WT-SP*): Balb/c mice were irradiated with 8 Gy and

Correspondence: Dr K Ozaki, Division of Hematology, Department of Medicine, Jichi Medical University, 3311-1 Yakushiji , Shimotsuke-shi, Tochigi, 329-0498, Japan.
E-mail: ozakikat@jichi.ac.jp
Received 20 April 2009; revised and accepted 6 July 2009; published online 31 August 2009

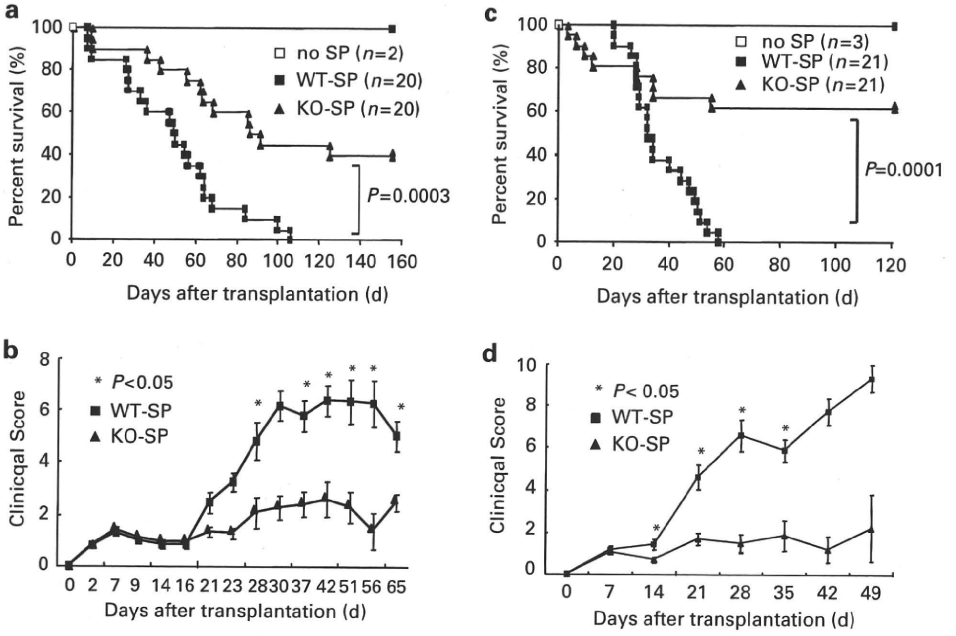

Figure 1 IL-21R$^{-/-}$ (knockout (KO)) splenocytes (SPs) ameliorated GVHD. (**a** and **b**) Survival and clinical score of GVHD with BM cells from wild type (WT) C57BL/6 mice (WT-BM). Balb/c recipients were transplanted with 5×10^6 WT-BM and either 5×10^6 SPs from WT or IL-21R KO C57BL/6 mice (KO-SP) or WT-SP. Open squares ($n = 2$), filled squares ($n = 20$) and filled triangles ($n = 20$) indicate transplants without SPs as controls, with WT-SP, and with IL-21R KO-SP, respectively. The combined results of three independent experiments are shown. *P*-values were calculated by the log-rank method. (**c** and **d**) Survival and clinical score of GVHD with IL-21R KO-BM. Balb/c recipients were transplanted with 5×10^6 IL-21R KO-BM and either 5×10^6 IL-21R KO-SP or WT-SP. Open squares ($n = 3$), filled squares ($n = 21$) and filled triangles ($n = 21$) indicate transplants without SPs as controls, with WT-SP, and with IL-21R KO-SP, respectively. The combined results of three independent experiments are shown. *P*-values were calculated by the log-rank method.

injected intravenously with 5×10^6 wild type (WT)-BM and 5×10^6 splenocytes (SPs) from either WT or KO mice.

GVHD group 2 (KO-BM and KO-SP vs *KO-BM and WT-SP)*: To delete the contaminated WT T cells in BM, we used KO-BM.

Flow cytometric analysis

Fc-block (BD Biosciences-Pharmingen, San Diego, CA, USA) was used to prevent non-specific Ab binding to Fc receptors. Anti-CD4, CD8, H-2^b and H-2^d Abs were purchased from BD Biosciences-Pharmingen. A LSR flow cytometer (BD Biosciences-Immunocytometry Systems, San Jose, CA, USA) was used for data collection, and the data were analyzed using CellQuest software (BD Biosciences-Immunocytometry Systems).

Decoy receptor of IL-21

The primers, 5′-TTCTAGCTACCAGCTGCAGGT-3′ and 5′-TCCTGAAGTTCCTCATATTCA-3′, were used to produce a truncated IL-21R lacking the region from box 1 to the C-terminus.[8] All nucleotide sequences were confirmed by sequencing. Extracellular expression of this receptor was confirmed by flow cytometric analysis using anti-IL-21-receptor polyclonal Ab (R&D Systems, Minneapolis, MN, USA) and a secondary Ab conjugated with FITC (R&D Systems).

Table 1 Donor CD4$^+$/CD8$^+$ T-cell numbers in spleen at day 14 after transplantation

	CD4$^+$	*CD8*$^+$
WT spleen ($n = 6$)	2.9 ± 1.2^a	3.2 ± 1.3^a
KO spleen ($n = 10$)	3.7 ± 1.1^a	3.3 ± 1.2^a
P-value	NS	NS

Abbreviations: KO = knockout; NS = not significant ($P \geqslant 0.05$) by Student's *t*-test; WT = wild type.
[a]Mean ± s.e.m. ($\times 10^{-6}$) from three independent experiments.

Retrovirus mediated transduction into BM

A retrovirus construct containing the decoy receptor of IL-21 was transfected into the packaging cell line, PLAT-E, and the viruses produced were transduced into pre-stimulated BM cells using Retronectin according to the manufacturer's instructions (Takara, Osaka, Japan). We used $5–15 \times 10^5$ BM cells from 5-FU injected mice at the beginning of cultivation.

Carboxyfluorescein diacetate succinimidyl ester staining

Splenocytes were stained with carboxyfluorescein diacetate succinimidyl ester (CFSE) for 15 min in phosphate-buffered saline, washed and injected into irradiated mice. Staining was carried out according to the manufacturer's instructions (Invitrogen-Molecular prove, Carlsbad, CA, USA).

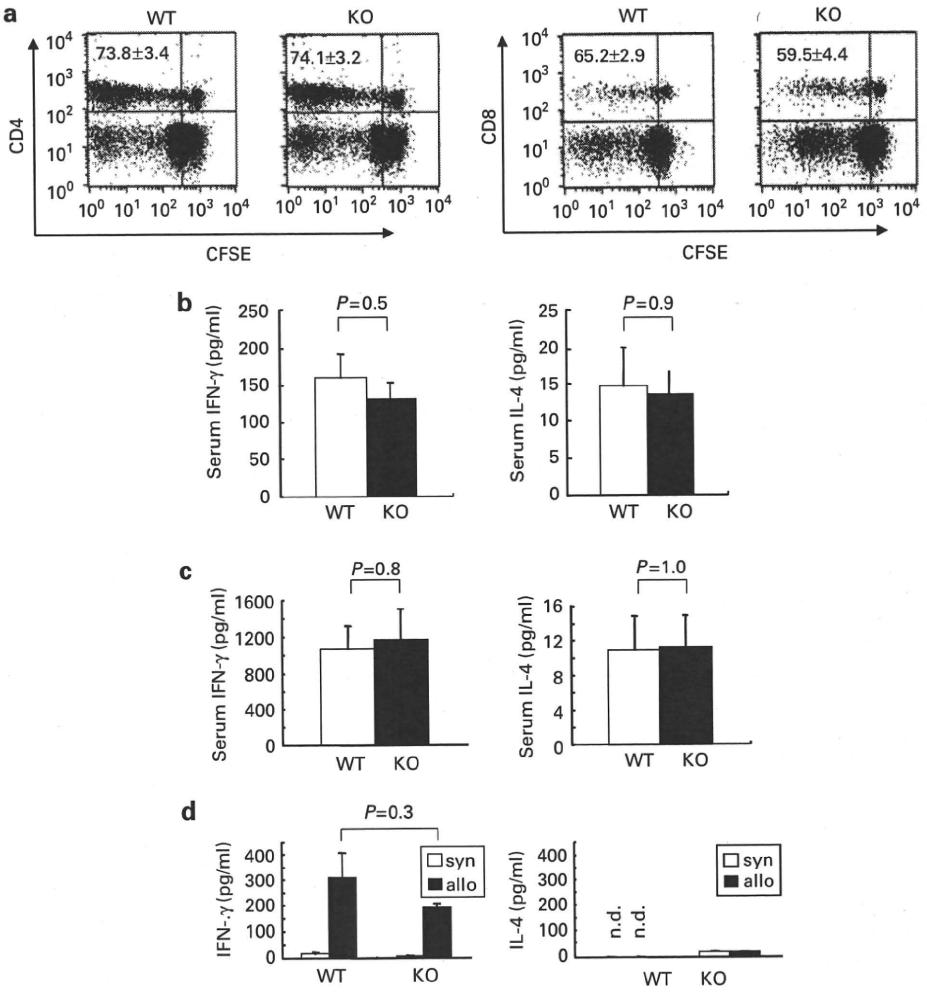

Figure 2 Proliferation and cytokine production after transplantation. (**a**) Flow cytometric analysis of CD4/CD8 proliferation *in vivo* by carboxyfluorescein diacetate succinimidyl ester (CFSE) staining. Splenocytes (SPs) (H-2^b 1×10^8) from either wild type (WT) or IL-21R knockout (KO) mice were stained with CFSE and transplanted into irradiated Balb/c mice; three days later, SPs were collected and analyzed. Donor cells were selected by gating on H-2^{d-}. The numbers at left quadrants were the percentage of dividing cells in CD4 or CD8 cells (mean ± s.e.m.). Total number of recipients analyzed was six mice in each group. (**b**) Serum cytokine concentrations at day 14 after transplantation. Balb/c recipients were transplanted with 5×10^6 IL-21R KO-BM and either 5×10^6 IL-21R KO-SP or WT-SP. Serum was sampled at day 14 after transplantation, and cytokine concentrations of IFN-γ (left panel) and IL-4 (right panel) were determined by ELISA. Total number of recipients analyzed was more than six mice in each group. (**c**) Serum cytokine concentrations at day 6 after transplantation. C57BL/6-DBA2 F1 recipients were transplanted with 1×10^8 SPs from WT or IL-21R KO mice. Serum was sampled at day 6 after transplantation, and cytokine concentrations of IFN-γ (left panel) and IL-4 (right panel) were determined by ELISA. Total number of recipients analyzed was five mice in each group. (**d**) Transplantations were carried out as in (**c**). At day 6, SPs (1×10^5) from recipients of WT-SP or IL-21R KO-SP were incubated with 30 Gy irradiated 4×10^5 SPs from C57BL/6 (syngeneic) or C57BL/6-DBA2 F1 (allogeneic) mice. After 72 h, cytokine concentrations in the supernatants were determined by ELISA. Total number of recipients analyzed was five mice in each group.

ELISA

Enzyme linked immunosorbent assay kits for cytokines, IFN-γ and IL-4 were purchased from BD Bioscience or R&D Systems. Concentrations were determined according to the manufacturer's instructions.

Statistical analysis

Kaplan–Meier plots were used to compare survival rates. The log-rank test was used to evaluate *P* values. The Mann–Whitney *U* test was used to calculate *P* values for the GVHD clinical score. Statistical analyses were performed using "Stat Mate ver. 6" (ATMS, Tokyo, Japan). Unless otherwise specified, all error bars in this study are s.e.m.

Results

IL-21R$^{-/-}$ SPs (KO-SP) cause attenuated GVHD with WT-BM

A well-established MHC-mismatch CD4 T cell-mediated GVHD model, C57BL/6 (H-2^b) → Balb/c (H-2^d), was used to evaluate the role for IL-21 in GVHD. BM cells and SPs were taken from donor C57BL/6 WT or IL-21R KO mice

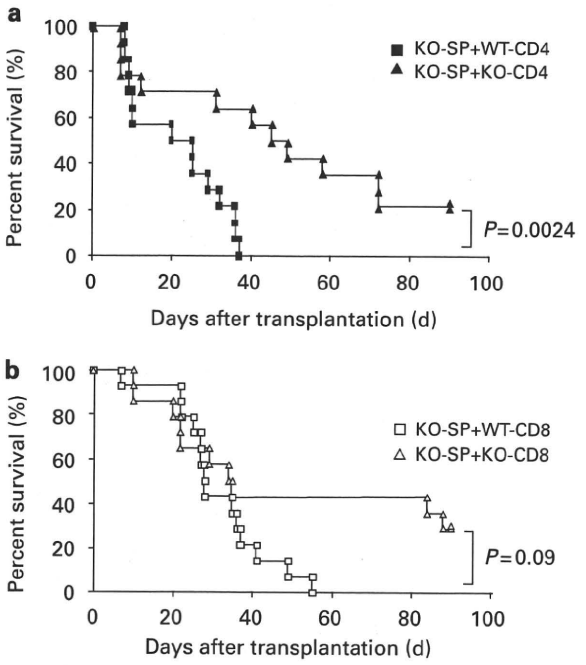

Figure 3 Effects of additional CD4 or CD8 T cells on survival. (**a**) Survival curve with addition of either wild type (WT)- or IL-21R knockout (KO)-CD4 cells. Transplantations were carried out as in Figure 1c. CD4 T cells (5×10^5) from either WT or KO mice were transplanted concomitantly with KO-BM (5×10^6) and KO-splenocyte (SP) (5×10^6). (**b**) Survival curve with addition of either WT- or IL-21R KO-CD8 cells. CD8 T cells (5×10^5) from either WT or IL-21R KO mice were transplanted with IL-21R KO-BM (5×10^6) and IL-21R KO-SP (5×10^6). The combined results of three independent experiments are shown. *P*-value was calculated by log-rank method.

and transplanted into irradiated Balb/c mice. Recipients of BM and SPs from WT mice became ill after 3–4 weeks and suffered from diarrhea, ruffled hair, a hunched posture and diminished body weight. In contrast, mice transplanted from IL-21R KO mice showed attenuated GVHD symptoms and survived longer (Figure 1a, $P=0.0003$, log-rank test). Strikingly, no mouse receiving the WT-SPs group survived more than 4 months, whereas 40% of the mice receiving the IL-21R KO SPs survived for 4 months or longer. Consistent with this, clinical GVHD scores in mice transplanted from IL-21R KO-SPs were significantly less than those in controls (Figure 1b). In both groups, approximately 85% engraftment in peripheral blood was achieved, indicating that the difference was not attributable to a difference in engraftment.

KO-SP causes attenuated GVHD when combined with KO-BM

In the preceding experiments (Figures 1a and b), we used unfractionated WT-BM, which presumably contained IL-21R-expressing T cells that could respond to IL-21. To eliminate contaminating IL-21R$^{+/+}$ T cells from BM, we next used BM from IL-21R KO mice, in combination with SPs from either WT or KO mice. This resulted in enhanced differences in survival between the groups receiving the WT vs IL-21R KO-SP after two months: 0 vs 60% (Figure 1c, $P=0.0001$ by log-rank test), respectively, confirming the former results (Figures 1a and b) and a critical role for IL-21 in GVHD. Consistent with this, clinical GVHD scores in the WT-SP group were higher than those in the IL-21R KO-SP group (Figure 1d).

CD4/CD8 proliferation and serum cytokine levels

To investigate the mechanisms underlying the attenuated GVHD in IL-21R KO-SP transplanted mice, we first counted the number of CD4 and CD8 cells in the spleens 14 days after transplantation. In both IL-21R KO-SP and WT-SP transplanted mice, both cell types were similar in number (Table 1). Next, SPs were stained with carboxyfluorescein diacetate succinimidyl ester to determine their proliferation in mice after transplantation. Both CD4 and CD8 cells from either WT-SP or IL-21R KO-SP transplanted mice showed similar proliferation profiles at day 3 (Figure 2a). Serum concentrations of IFN-γ and IL-4 at day 14 (Figure 2b), those at day 6 (Figure 2c), and IFN-γ and IL-4 produced by recipients' SPs stimulated with allogeneic SPs *in vitro* were comparable between two groups (Figure 2d).

Effects of additional CD4 or CD8 cells on survival

To investigate whether CD4$^+$ T cells are more important for GVHD than CD8$^+$ T cells in our system, we added either WT-CD4$^+$ or IL-21R KO-CD4$^+$ T cells onto the result-predictable transplantation with IL-21R KO-BM and IL-21R KO-SP (Figure 1c). The addition of WT-CD4$^+$ cells resulted in a significantly worse survival than seen with the addition of IL-21R KO-CD4$^+$ cells (Figure 3a, $P=0.0024$, log-rank method). In contrast to this, the difference between WT-CD8$^+$ and IL-21R KO-CD8$^+$ T cells did not reach statistical significance (Figure 3b, $P=0.09$, log-rank method), although they have similar tendency, suggesting that WT-CD4$^+$ rather than WT-CD8$^+$ cells is more important for GVHD, at least in our conditions.

A decoy receptor of IL-21 ameliorates GVHD

To develop a treatment or prophylaxis model in mice and exclude the possibility that the ameliorated GVHD is due to an intrinsic defect in the IL-21R KO-SPs, we designed a decoy receptor of IL-21, which contains its signal sequence, extracellular domain and transmembrane domain, but a truncated intracellular domain. The cDNA encoding this truncated IL-21R was produced by PCR, sequenced, and its extracellular expression in 293 cells was confirmed by flow cytometric analysis using an anti-IL-21R Ab (Figure 4a). In 293 cells, we confirmed that the IL-21R decoy reduced IL-21 concentration in the medium *in vitro* (Figure 4b). Using retroviral transduction, we expressed the decoy receptor in IL-21R KO-BM cells and transplanted them concomitantly with WT-SPs. We carried out three independent experiments and evaluated the survival. Two weeks after transplantation, transduction efficiencies were determined in peripheral blood by measuring green fluorescent protein-positive cells, and were found to be approximately 30–70% (Figure 4c). In an additional experiment, in which transduction efficiency was 40%, the serum concentration of IL-21 was not detectable in decoy receptor transduced BM recipients, whereas those trans-

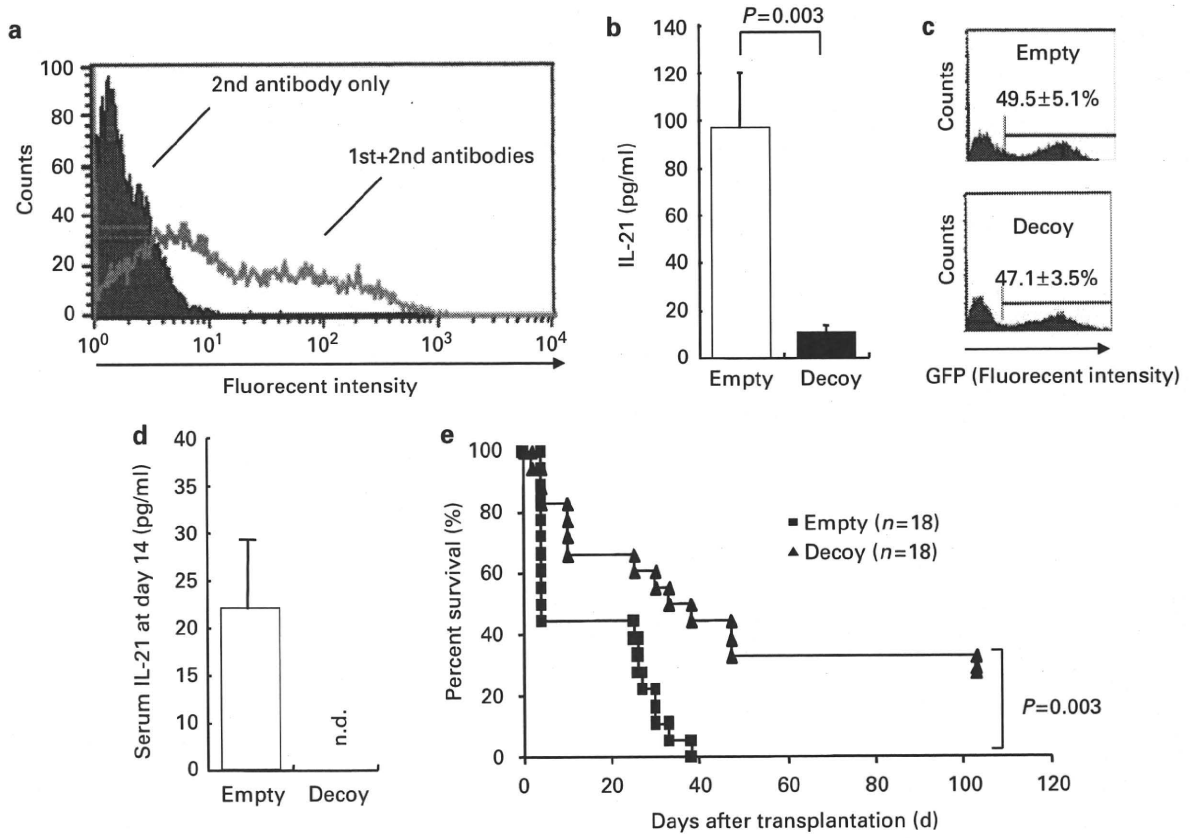

Figure 4 Forced expression of IL-21 decoy receptor ameliorated GVHD. (**a**) Expression of the IL-21 decoy receptor in the 293 cells. (**b**) *In vitro* activity of IL-21 decoy receptor. In all, 293 cells were transduced with either the IL-21 decoy receptor or empty vector, and then recombinant mouse IL-21 (1000 pg/ml) was added to the medium. IL-21 levels were determined by ELISA after 18 h. Shown is mean ± s.d. from three independent experiments ($P = 0.003$). (**c**) Transduction efficiency in peripheral blood 2 weeks after transplantation. Transduction efficiency was determined by flow cytometric analysis. Transduced cells are green fluorescent protein (GFP)-positive as the vector contains internal ribosomal entry site (IRES)-GFP. (**d**) Serum concentration of IL-21 at day 14 after transplantation. In this particular experiment, transduction efficiency was approximately 40% in both groups. Total mice analyzed were four empty vector transduced BM recipients and five decoy receptor transduced BM recipients. (**e**) Survival curve after forced expression of the IL-21 decoy receptor. Balb/c recipients were irradiated with 8 Gy and transplanted with wild type splenocytes (5×10^6) and either empty-vector or decoy-receptor transduced BM (starting dose at 5×10^5). Filled squares and filled triangles indicate transplantions with empty-vector transduced BM ($n = 18$) and decoy-receptor transduced BM ($n = 18$), respectively. The combined results of three independent experiments are shown ($P = 0.003$, log-rank test).

duced with the empty vector showed 22 pg/ml on average (Figure 4d), indicating that the decoy receptor significantly diminished serum IL-21 *in vivo*. Although most of the expression was transient, decoy IL-21R-transduced BM resulted in prolonged survival compared with empty-vector transduced BM (Figure 4e, $P = 0.003$, log-rank test), suggesting that blockade of the IL-21 signal might be an effective treatment or prophylaxis for GVHD. These results are consistent with the results shown above (Figure 1), and support the hypothesis that IL-21 promotes GVHD.

The attenuated GVHD appeared to be independent of cytotoxic molecules

The significance of cytotoxic molecules such as perforin and granzyme B in GVHD has been reported.[24] To investigate the relationship between these molecules and the attenuated GVHD, we sought to see the levels of expression of these molecules in $CD4^+$ and $CD8^+$ T cells. No clear difference between WT-SP and IL-21R KO-SP transplanted mice was detected (Figure 5a). Moreover, we used a combination of IL-21 decoy receptor and *perforin*-deficient mice. The IL-21 decoy receptor-transduced BM improved survival of recipients with SPs from *perforin*-deficient mice, suggesting that the mechanism of the attenuated GVHD is primarily independent of perforin *in vivo* (Figure 5b). The Fas/FasL system is another cytotoxic molecule and was reported to be important for GVHD rather than GVL.[25,26] To investigate a possible role for Fas/FasL in the attenuated GVHD, we analyzed the effect of IL-21 decoy receptor transduced BM on survival of recipients with SPs from FasL deficient (*gld/gld*) mice and found enhanced survival, suggesting that the mechanism of the attenuated GVHD is also primarily independent of Fas/FasL (Figure 5c).

Discussion

Here, we report that IL-21 is critical for GVHD. SPs from IL-21R$^{-/-}$ (KO) mice induced less severe GVHD than those from WT mice. Moreover, a decoy receptor for IL-21 attenuates GVHD and prolongs survival, confirming the

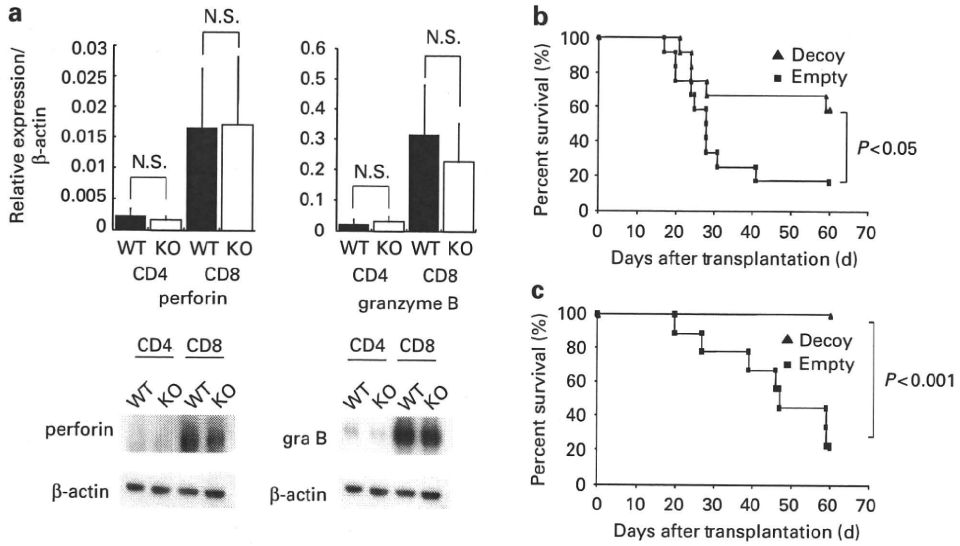

Figure 5 The ameliorated GVHD is dependent on neither FasL nor perforin. (**a**) Perforin and granzyme B expression in CD4/CD8 cells. C57BL/6-DBA2 F1 recipients were transplanted with 1×10^8 splenocytes (SPs) from wild type or IL-21R$^{-/-}$ mice. tRNA and protein were harvested from CD4 or CD8 cells purified from transplanted mice at day 6 after transplantation. Results of RT-qPCR and western blot analysis are shown in upper and lower panel, respectively. (**b**) Survival curve with SPs from perforin deficient mice. C57BL/6-DBA2 F1 recipients were irradiated with 11 Gy and transplanted with either empty-vector or decoy-receptor transduced BM (final cell number: $3–3.2 \times 10^6$) with SPs from perforin-deficient mice ($3.75–5 \times 10^7$). Filled squares and filled triangles indicate transplantations with empty-vector transduced BM ($n=9$) or decoy-receptor transduced BM ($n=9$), respectively. The combined results of two independent experiments are shown. *P*-value was calculated by the log-rank method. Transduction efficiencies two weeks after transplantation in peripheral blood were around 30–70% like Figure 4c. (**c**) Survival curve with SPs from FasL deficient mice (*gld*/*gld* mice). C57BL/6-DBA2 F1 recipients were irradiated with 11 Gy and transplanted with either empty-vector or decoy-receptor transduced BM (final cell number: $3.2–3.5 \times 10^6$) with SPs from *gld*/*gld* mice ($8–10 \times 10^7$). Filled squares and filled triangles indicate transplantations with empty-vector transduced BM ($n=12$) or decoy-receptor transduced BM ($n=12$), respectively. The combined results of two independent experiments are shown. The *P*-value was calculated by the log-rank method.

former experiments with KO mice and suggesting that a possible clinical application of blocking IL-21 for the treatment or prophylaxis of GVHD.

Serum IFN-γ and IL-4 concentrations, CD4/CD8 T-cell proliferation at day 3 after transplantation, and the number of CD4$^+$/CD8$^+$ T cells in spleens of recipients at day 14 after transplantation, all appeared to be comparable between two groups at least under the conditions we have tested. In addition, the decoy IL-21R also ameliorated GVHD induced by *FasL*-deficient and *perforin*-deficient SPs, suggesting that Fas/FasL and perforin are not crucial for the mechanism of the attenuated GVHD by IL-21R KO SPs. However, we could not rule out the possibility that the other transplantation conditions might make the difference more profound and lead to interpretation of the mechanisms. Results of additional CD4$^+$/CD8$^+$ experiments suggested the importance of CD4$^+$ cells. We are now investigating the process by using other transplantation models, such as purified CD4$^+$ T-cell transplantation.

Although we have shown that IL-21 is critical for GVHD in two different systems using both IL-21R KO mice and decoy receptor for IL-21, the molecular mechanisms by which blocking IL-21 attenuates GVHD are not clear at this point.

As the transplantation model we used is an MHC-mismatch CD4$^+$ cell-mediated GVHD, a role for IL-21 in both CD8$^+$ cell-mediated GVHD and MHC-matched GVHD is an area for future investigation.

Here, we opened a new insight for mechanisms of GVHD. These results would help in understanding the mechanisms of GVHD and in developing a treatment for GVHD. In fact, we could demonstrate that IL-21 blockade is a potentially novel approach for the treatment or prophylaxis of GVHD in mouse model. Further *in vivo* and *in vitro* studies, including humans, are required to potentially translate these results from mouse models to human diseases.

Conflict of interest

Drs Katsutoshi Ozaki and Warren J Leonard are inventors on patents and patent applications related to IL-21.

Acknowledgements

We thank Dr Kitamura (Institute of Medical Science, University of Tokyo, Tokyo) for donating PLAT-E, a packaging cell line. This work was supported in part by grants from the Ministry of Health, Labor and Welfare of Japan, by Grants-in-Aid for Scientific Research from the Ministry of Education, Culture, Sports, Science and Technology of Japan, by the Intramural Research Program of the National Heart, Lung and Blood Institute, National Institutes of Health (Bethesda, MD, USA), and by an Intramural Research Grant from Jichi Medical University, Tochigi, Japan.

References

1 Ozaki K, Leonard WJ. Cytokine and cytokine receptor pleiotropy redundancy. *J Biol Chem* 2002; **277**: 29355–29358.

2 Leonard WJ. Cytokines immunodeficiency diseases. *Nat Rev Immunol* 2001; **1**: 200–208.
3 Noguchi M, Yi H, Rosenblatt HM, Filipovich AH, Adelstein S, Modi WS *et al.* Interleukin-2 receptor gamma chain mutation results in X-linked severe combined immunodeficiency in humans. *Cell* 1993; **73**: 147–157.
4 von Freeden-Jeffry U, Vieira P, Lucian LA, McNeil T, Burdach SE, Murray R. Lymphopenia in interleukin (IL)-7 gene-deleted mice identifies IL-7 as a nonredundant cytokine. *J Exp Med* 1995; **181**: 1519–1526.
5 Lodolce JP, Boone DL, Chai S, Swain RE, Dassopoulos T, Trettin S *et al.* IL-15 receptor maintains lymphoid homeostasis by supporting lymphocyte homing and proliferation. *Immunity* 1998; **5**: 669–676.
6 Ozaki K, Spolski R, Feng CG, Qi CF, Cheng J, Sher Au C *et al.* A critical role for IL-21 in regulating immunoglobulin production. *Science* 2002; **298**: 1630–1634.
7 Parrish-Novak J, Dillon SR, Nelson A, Hammond A, Sprecher C, Gross JA *et al.* Interleukin 21 and its receptor are involved in NK cell expansion and regulation of lymphocyte function. *Nature* 2000; **408**: 57–63.
8 Ozaki K, Kikly K, Michalovich D, Young PR, Leonard WJ. Cloning of a type I cytokine receptor most related to the IL-2 receptor beta chain. *Proc Natl Acad Sci USA* 2000; **97**: 11439–114344.
9 Brandt K, Bulfone-Paus S, Foster DC, Ruckert R. Interleukin-21 inhibits dendritic cell activation and maturation. *Blood* 2003; **102**: 4090–4098.
10 Ozaki K, Hishiya A, Hatanaka K, Nakajima H, Wang G, Hwu P *et al.* Overexpression of IL-21 induces expansion of hematopoietic progenitor cells. *Int J Hemat* 2006; **84**: 224–230.
11 Zhou L, Ivanov II, Spolski R, Min R, Shenderov K, Egawa T *et al.* IL-6 programs T(H)-17 cell differentiation by promoting sequential engagement of the IL-21 and IL-23 pathways. *Nat Immunol* 2007; **8**: 967–974.
12 Nurieva R, Yang XO, Martinez G, Zhang Y, Panopoulos AD, Ma L *et al.* Essential autocrine regulation by IL-21 in the generation of inflammatory T cells. *Nature* 2007; **448**: 480–483.
13 Korn T, Bettelli E, Gao W, Awasthi A, Jäger A, Strom TB *et al.* IL-21 initiates an alternative pathway to induce proinflammatory T(H)17 cells. *Nature* 2007; **448**: 484–487.
14 Wurster AL, Rodgers VL, Satoskar AR, Whitters MJ, Young DA, Collins M *et al.* Interleukin 21 is a T helper (Th) cell 2 cytokine that specifically inhibits the differentiation of naive Th cells into interferon gamma-producing Th1 cells. *J Exp Med* 2002; **196**: 969–977.
15 Pesce J, Kaviratne M, Ramalingam TR, Thompson RW, Urban Jr JF, Cheever AW *et al.* The IL-21 receptor augments Th2 effector function and alternative macrophage activation. *J Clin Invest* 2006; **116**: 2044–2055.
16 Fröhlich A, Marsland BJ, Sonderegger I, Kurrer M, Hodge MR, Harris NL *et al.* IL-21 receptor signaling is integral to the development of Th2 effector responses *in vivo*. *Blood* 2007; **109**: 2023–2031.
17 Strengell M, Sareneva T, Foster D, Julkunen I, Matikainen S. IL-21 up-regulates the expression of genes associated with innate immunity and Th1 response. *J Immunol* 2002; **169**: 3600–3605.
18 Ozaki K, Spolski R, Ettinger R, Kim HP, Wang G, Qi CF *et al.* Regulation of B cell differentiation and plasma cell generation by IL-21, a novel inducer of Blimp-1 and Bcl-6. *J Immunol* 2004; **173**: 5361–5371.
19 Bubier JA, Sproule TJ, Foreman O, Spolski R, Shaffer DJ, Morse III HC *et al.* A critical role for IL-21 receptor signaling in the pathogenesis of systemic lupus erythematosus in BXSB-Yaa mice. *Proc Natl Acad Sci USA* 2009; **106**: 1518–1523.
20 Spolski R, Kashyap M, Robinson C, Yu Z, Leonard WJ. IL-21 signaling is critical for the development of type I diabetes in the NOD mouse. *Proc Natl Acad Sci USA* 2008; **105**: 14028–14033.
21 Sutherland AP, Van Belle T, Wurster AL, Suto A, Michaud M, Zhang D *et al.* IL-21 is required for the development of type 1 diabetes in NOD mice. *Diabetes* 2009; **58**: 1144–1155.
22 Shlomchik WD. Graft-versus-host disease. *Nat Rev Immunol* 2007; **7**: 340–352.
23 Cooke KR, Kobzik L, Martin TR, Brewer J, Delmonte Jr J, Crawford JM *et al.* An experimental model of idiopathic pneumonia syndrome after bone marrow transplantation: I. The roles of minor H antigens and endotoxin. *Blood* 1996; **88**: 3230–3239.
24 Graubert TA, DiPersio JF, Russell JH, Ley TJ. Perforin/granzyme-dependent and independent mechanisms are both important for the development of graft-versus-host disease after murine bone marrow transplantation. *J Clin Invest* 1997; **100**: 904–911.
25 Tsukada N, Kobata T, Aizawa Y, Yagita H, Okumura K. Graft-versus-leukemia effect and graft-versus-host disease can be differentiated by cytotoxic mechanisms in a murine model of allogeneic bone marrow transplantation. *Blood* 1999; **93**: 2738–2747.
26 Schmaltz C, Alpdogan O, Horndasch KJ, Muriglan SJ, Kappel BJ, Teshima T *et al.* Differential use of Fas ligand and perforin cytotoxic pathways by donor T cells in graft-versus-host disease and graft-versus-leukemia effect. *Blood* 2001; **97**: 2886–2895.

ELSEVIER

Experimental Hematology

Experimental Hematology 2009;37:1250–1257

Cotransplantation with MSCs improves engraftment of HSCs after autologous intra-bone marrow transplantation in nonhuman primates

Shigeo Masuda[a], Naohide Ageyama[b], Hiroaki Shibata[b], Yoko Obara[c], Tamako Ikeda[a], Kengo Takeuchi[d], Yasuji Ueda[e], Keiya Ozawa[c], and Yutaka Hanazono[a]

[a]*Division of Regenerative Medicine, Center for Molecular Medicine, Jichi Medical University, Tochigi, Japan;* [b]*Tsukuba Primate Research Center, National Institute of Biomedical Innovation, Ibaraki, Japan;* [c]*Division of Hematology, Department of Medicine, Jichi Medical University, Tochigi, Japan;* [d]*Division of Pathology, The Cancer Institute, Tokyo, Japan;* [e]*Department of Gene Therapy, Graduate School of Medicine, Chiba University, Chiba, Japan*

(Received 18 June 2009; revised 21 July 2009; accepted 22 July 2009)

Objective. **Hematopoietic stem cells (HSCs) reside in the osteoblastic niche, which consists of osteoblasts. Mesenchymal stromal cells (MSCs) have an ability to differentiate into osteoblasts. Here, using nonhuman primates, we investigated the effects of cotransplantation with MSCs on the engraftment of HSCs after autologous intra-bone marrow transplantation.**

Materials and Methods. **From three cynomolgus monkeys, CD34-positive cells (as HSCs) and MSCs were obtained. The former were divided into two equal aliquots and each aliquot was genetically marked with a distinctive retroviral vector to track the in vivo fate. Each HSC aliquot with or without MSCs was autologously injected into the bone marrow (BM) cavity of right or left side, enabling the comparison of in vivo fates of the two HSC grafts in the same body.**

Results. **In the three monkeys, $CD34^+$ cells transplanted with MSCs engrafted 4.4, 6.0, and 1.6 times more efficiently than $CD34^+$ cells alone, as assessed by BM colony polymerase chain reaction. In addition, virtually all marked cells detected in the peripheral blood were derived from the cotransplantation aliquots. Notably, colony-forming units derived from the cotransplantation aliquots were frequently detected in BM distant sites from the injection site, implying that cotransplantation with MSCs also restored the ability of gene-marked HSCs to migrate and achieve homing in the distant BM.**

Conclusion. **Cotransplantation with MSCs would improve the efficacy of transplantation of gene-modified HSCs in primates, with enhanced engraftment in BM as well as increased chimerism in peripheral blood through migration and homing.** © **2009 ISEH - Society for Hematology and Stem Cells. Published by Elsevier Inc.**

Hematopoietic stem cells (HSCs) have been shown to reside in the hematopoietic niche, such as the osteoblastic or vascular niche [1,2]. The osteoblastic niche is provided by bone marrow (BM) osteoblasts, which are derived from mesenchymal stromal cells (MSCs) [3–5]. Although conditioning, such as total body irradiation or administration of busulfan, would be required for successful engraftment of transplanted HSCs, the treatment may destroy the osteoblastic niche, hampering engraftment [6]. If an osteoblastic niche could be generated through cotransplantation with MSCs, the engraftment of HSCs would be enhanced; however, MSCs cannot home to or engraft in BM when transplanted via vessels [7]. On the other hand, the direct transplantation of HSCs into a BM cavity, namely intra-bone marrow transplantation (iBMT), improves engraftment of HSCs compared with intravascular transplantation [8–13]. In fact, one clinical trial of iBMT has been published recently [14] that demonstrates early donor engraftment

Offprint requests to: Yutaka Hanazono, M.D., Ph.D., Division of Regenerative Medicine, Center for Molecular Medicine, Jichi Medical University, 3311-1 Yakushiji, Shimotsuke-shi, Tochigi 329-0498, Japan; E-mail: hanazono@jichi.ac.jp

Supplementary data associated with this article can be found, in the online version, at doi:10.1016/j.exphem.2009.07.008.

0301-472X/09 $–see front matter.
doi: 10.1016/j.exphem.2009.07.008